

Goodrich, D. C., Williams, D. G., Unkrich, C. L., Hogan, J. F., Scott, R. L., Hultine, K. R., Pool, D., Coes, A. L., Miller, S. N. 2004. Comparison of Methods to Estimate Ephemeral Channel Recharge, Walnut Gulch, San Pedro River Basin, Arizona. In Recharge and Vadose Zone Processes: Alluvial Basins of the Southwestern United States, ed. by F.M. Phillips, J.F. Hogan, and B. Scanlon, Water Science and Application 9, Washington, DC, American Geophysical Union, p. 77-99. 2004.

Comparison of Methods to Estimate Ephemeral Channel Recharge, Walnut Gulch, San Pedro River Basin, Arizona

David C. Goodrich¹, David G. Williams⁵, Carl L. Unkrich¹, James F. Hogan⁴, Russell L. Scott¹, Kevin R. Hultine², Don Pool³, Alissa L. Coes³, Scott Miller⁵

Ephemeral channel transmission loss represents an important groundwater-surface water exchange in arid and semiarid regions and is potentially a significant source of recharge at the basin scale. However, identification of the processes and dynamics that control this exchange is a challenging problem. Specifically, data on the proportion of runoff transmission losses that escape from near-channel transpiration and wetted channel evaporation to become deep groundwater recharge are difficult to obtain. This issue was addressed through coordinated field research and modeling within the USDA-ARS Walnut Gulch Experimental Watershed (WGEW) located in the San Pedro River Basin of southeastern Arizona. Recharge was estimated using several independent methods which included a reach water balance approach, with near-channel ET estimated using sap flux and micrometeorological measurements; geochemical methods such as chloride mass balance; modeling of changes in groundwater level or microgravity measurements; and vadose zone water and temperature transport modeling. It was found that during the relatively wet 1999 and average 2000 monsoon seasons, the range of ephemeral channel recharge estimated from these methods differed by a factor of less than three. A rough scaling to the entire San Pedro Basin indicates that ephemeral channel recharge constitutes between ~15% and ~40% of total annual recharge to the regional aquifer as estimated from a calibrated groundwater model. In contrast, during the weak monsoon seasons of 2001 and 2002 limited runoff and stream channel infiltration did occur but no discernable deep aquifer recharge was detected.

¹USDA-Agricultural Research Service, Southwest Watershed Research Center, Tucson, Arizona

²University of Arizona, School of Renewable Natural Resources, Tucson, Arizona

³U.S. Geological Survey, Tucson, Arizona

⁴University of Arizona, Department of Hydrology and Water Resources, Tucson, Arizona

⁵University of Wyoming, Department of Renewable Resources, Laramie, Wyoming

INTRODUCTION

Recharge estimates are essential for the sustainable management of groundwater resources, however recharge is arguably the water balance component known with the least certainty. Mounting evidence suggests that in arid and semiarid regions recharge likely occurs in only small portions of the basin where flow is concentrated, such as depressions and ephemeral stream channels; elsewhere little recharge occurs [Heilweil and Solomon, 2004; Plummer *et al.*, 2004; Scanlon *et al.*, 1997, 1999 & 2003; Scott *et al.*, 1999; Walvoord, 2002; Walvoord *et al.*, 2002]. Ephemeral channel transmission loss represents a significant water flux in semi-

2 COMPARISON OF METHODS TO ESTIMATE EPHEMERAL CHANNEL RECHARGE

arid and arid regions and therefore is potentially a significant source of groundwater recharge [Lane, 1983; Renard *et al.*, 1993; Goodrich *et al.*, 1997]. However, runoff water absorbed by the channel alluvium is subject to several abstractions before it contributes to deep aquifer recharge. Two relatively immediate abstractions are transpiration by near-channel vegetation and evaporation from the wetted channel. At longer timescales (> 5 days), impeding subsurface soil and geology may continue to retain channel transmission losses near the surface for vegetation transpiration or divert it downslope to areas of discharge or additional vegetation and subsequent transpiration.

While the measurement of transmission loss is straightforward, when accurate discharge measurements at both ends of the channel reach can be obtained, a number of interdisciplinary challenges must be met to quantify the proportion that escapes near-channel evapotranspiration (ET) and wetted channel evaporation to become groundwater recharge. A comprehensive review of ephemeral channel recharge and associated methods is contained within this monograph [Blasch *et al.*, 2004]. This paper addresses the issue of ephemeral channel recharge by:

- 1) comparing estimated ephemeral channel recharge using three fundamental types of approaches: a) closing the water balance for the channel reach by directly measuring near channel ET, b) measurement changes in groundwater volume directly (well levels) or indirectly (microgravity), and c) using geochemical tracers (chloride concentrations and oxygen isotopes) or geophysical tracers (temperature).
- 2) assessing the magnitude and annual variability of ephemeral channel recharge to the regional aquifer and determining the significance of this contribution to recharge at the basin scale.

STUDY SITE

This study was undertaken at the highly instrumented 148 km² USDA-ARS Walnut Gulch Experimental Watershed (WGEW) in southeastern Arizona, U.S.A. (31° 43'N, 110° 41'W) (Figure 1). WGEW is representative of approximately 60 million hectares of shrub and grass covered rangeland found throughout the Chihuahuan and Sonoran Deserts of the southwestern United States and northern Mexico. A detailed description of the watershed, its observational infrastructure, and a variety of the research that has been conducted there is contained in Renard *et al.* [1993]; only the relevant information is summarized below.

Mean annual precipitation is 324 mm, however precipitation varies substantially from year to year and from season to season. Roughly two-thirds of annual precipitation results from high intensity, convective thunderstorms of limited extent associated with the summer monsoon. The remaining one-third originates from low-intensity winter precipitation associated with cold fronts. Ephemeral channel runoff at the WGEW occurs almost exclusively during the summer season.

This study focuses on the channel reach in the middle and lower portion of the WGEW (between flumes 6, 2, and 1 on Figure 1). The areas drained by flumes 2, 6 and 7 are 112 km², 93.6 km² and 13.6 km² respectively. The supercritical flumes at WGEW were specifically designed to provide accurate runoff measurements in mobile channel beds composed of a coarse sand and gravel aggregate [Smith *et al.*, 1982]. The present-day channel is situated within the fill of an earlier secondary channel which ranges in width from roughly 13 m at flume 6 to 31 m at flume 1. The high porosity and rapid infiltration characteristics of the channel bed can result in significant transmission losses over the 11 km of channel between flume 6 and flume 1 [Renard *et al.*, 1993; Lane, 1983]. For example, the volume of transmission losses during an event on August 27, 1982 (Figure 2) equaled ~9% of the total annual recharge for the larger San Pedro Basin (4480 km²) as derived from a calibrated regional groundwater model [Corell *et al.*, 1996].

WGEW is underlain by very deep (>400 m) Cenozoic alluvium related to the high foothill alluvial fan portion of the larger San Pedro Basin. The alluvium consists of clastic materials ranging from clays and silts to well-cemented boulder conglomerates with little continuity of bedding. The alluvium constitutes a significant regional groundwater aquifer. Depth to groundwater within the WGEW ranges from ~50 m at the lower end to ~145 m in the central portion of the watershed. A shallow perched aquifer is present near flume 2, resulting in an appreciable concentration of streamside vegetation. This area was selected for detailed measurements to estimate near channel vegetation ET with the expectation that it represent the high extreme of near channel ET values. Thus, when ET is extrapolated to the entire reach, a conservatively low recharge estimate will be obtained.

Eight shallow wells within the perched aquifer system above flume 2 (Figure 1 – flume 2 inset) and four deep wells throughout the regional aquifer were instrumented with water level recorders in June 1999 to monitor groundwater levels before and after runoff events (Figure 1). Three deep wells are located in a transect above Flume 1 (Figure 1 – flume 1 inset). The wells were drilled in the late 1960s to

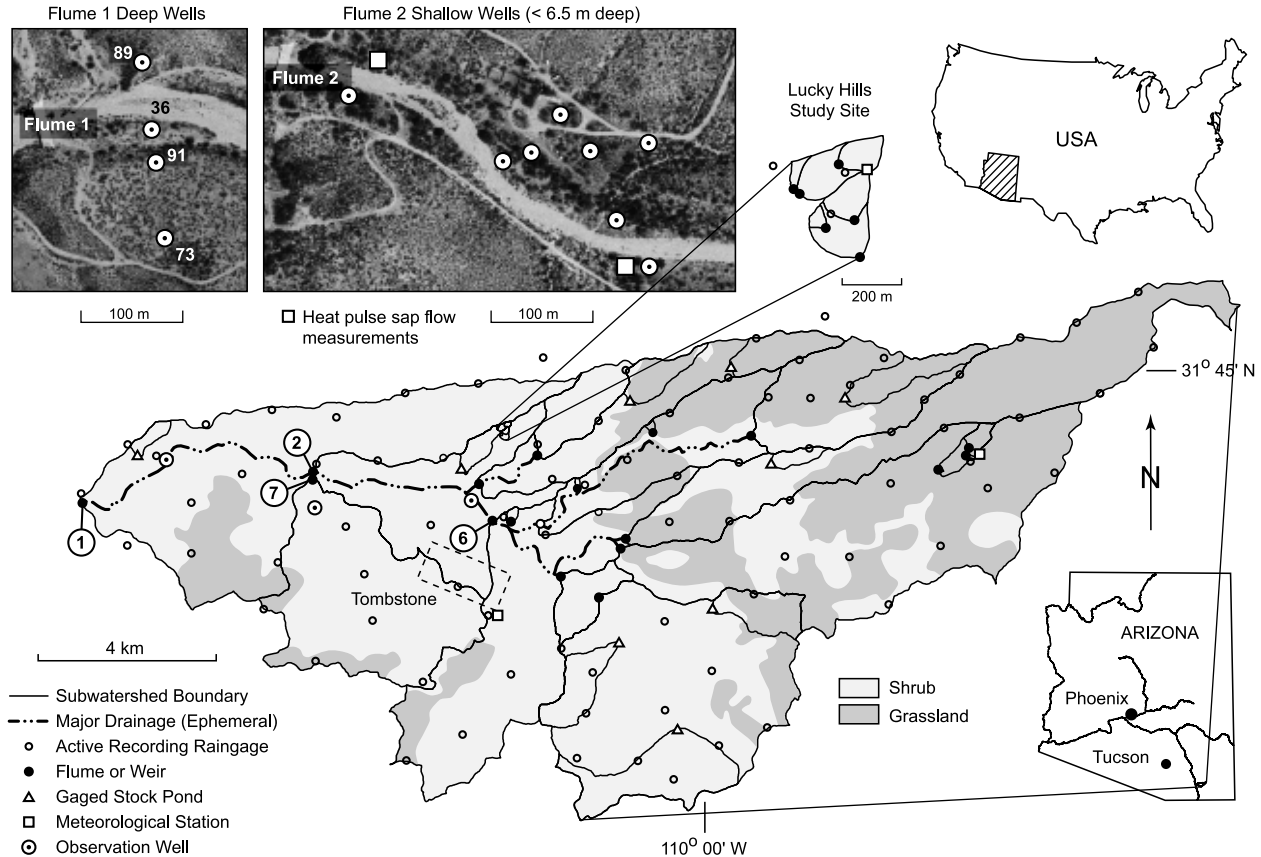


Figure 1. Walnut Gulch Experimental Watershed.

early 1970s and range in depth from 57.7 to 134.6 meters below the mid-channel elevation. The casings were slotted from a depth of 46.0 meters down to the bottom. The depth to water in July of 1999 was 48.2 meters.

METHODS AND MEASUREMENTS

In this study we estimate ephemeral channel recharge using the following methods: 1) channel reach water balance; 2) modeling of groundwater mounding [Hantush, 1967]; 3) microgravity measurements [Pool and Eychaner, 1995]; 4) geochemical tracers such as changes in chloride concentration or oxygen and hydrogen isotopes [Allison *et al.*, 1994]; and 5) vadose zone water and temperature transport modeling to estimate infiltration flux [Coes and Pool, in review]. Only the basic principles and relevant site-specific details of each method are provided below. Note that the intent of this paper is to compare across a variety of methods. In doing so, resources were not available to collect the necessary number of samples or data to conduct a

detailed uncertainty analysis in each method. A qualitative comparison of the methods is included which examines the factors or measurements with high degrees of uncertainty.

3.1. Channel Reach Water Balance

The water balance approach assumes that ephemeral channel recharge equals channel transmission losses less the abstractions from near channel vegetation transpiration and channel evaporation. Recharge (R) can be estimated using the following channel reach water balance:

$$R = Q_i + Q_l - Q_o + P - E - T + \Delta S \quad (1)$$

where:

- Q_i , Q_o are flume measured reach inflow and outflow;
- Q_l is lateral inflow estimated using KINEROS2 runoff modeling [Smith *et al.*, 1995];
- P is direct precipitation on the stream channel estimated from multiple raingages;

4 COMPARISON OF METHODS TO ESTIMATE EPHEMERAL CHANNEL RECHARGE

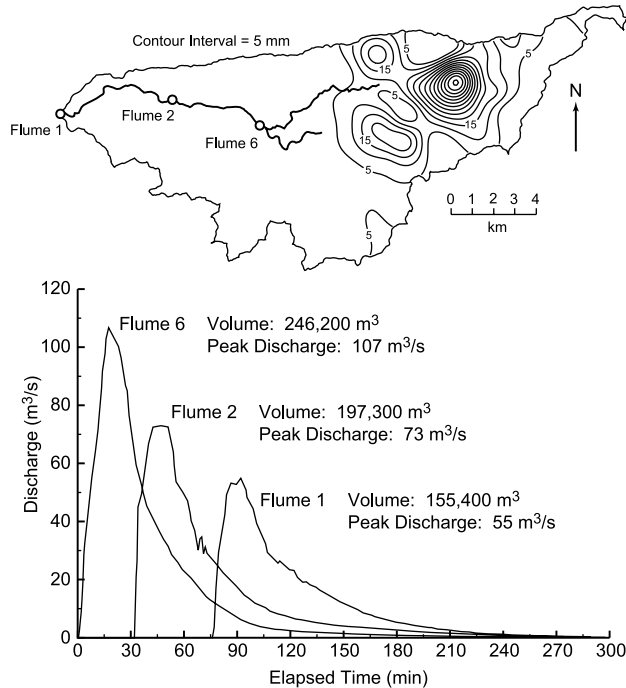


Figure 2. Transmission losses during a storm in the upper portion of WGEW on August 27, 1982.

- E is channel evaporation based on meteorological estimates [Sorey and Matlock, 1969];
- T is near-channel transpiration adjusted for interception, estimated by scaling sap flux measurements [Barrett et al., 1995] or energy flux estimated using micrometeorological techniques [Scott et al., 2003]; and,
- ΔS is the change in storage.

3.1.1 Lateral inflow and channel transmission losses. Channel transmission losses from the main channel stem between flumes 1 and 2 for 1999 and 2000 were calculated using measured flow volumes at flumes 1, 2, and 7 and lateral inflow into the main stem estimated using KINEROS2. KINEROS2 is a physically based runoff and erosion model [Woolhiser et al., 1990; Smith et al., 1995; Goodrich et al., 2002] that describes the processes of interception, infiltration, runoff generation, erosion, and sediment transport from agricultural and urban watersheds for individual rainfall-runoff events. Transmission losses were not directly calculated using KINEROS2. This avoided model routing through the main channel, potentially the largest source of modeling error.

The infiltration component of the KINEROS2 model is based on the Smith and Parlange [1978] simplification of the Richards equation, which assumes a semi-infinite, uni-

form soil for each model element. Runoff generated by infiltration excess is routed interactively using the kinematic wave equations for overland flow and channel flow. These equations are solved using a four-point implicit finite difference method (see Smith et al., [1995] for details). Interactive routing implies that infiltration and runoff are computed at each finite difference node, using rainfall, upstream inflow, and current degree of soil saturation. Unlike an excess routing scheme, infiltration can therefore continue after rainfall ceases if there is upstream inflow.

In KINEROS2, the lateral overland flow areas of the watershed (Figure 3) are abstracted in the model as rectangular overland flow model elements connected to open channels with trapezoidal cross sections. Digital orthophotos with a resolution of 0.5 meters were digitized to define the lengths and widths of the channel segments. The Automated Geospatial Watershed Assessment (AGWA) tool [Miller et al., 2002] generated area, length, and slope values for each overland model element and slopes for the channel elements. Hydraulic and infiltrative parameters were based on a previous model of the WGEW [Goodrich, 1990; Goodrich et al., 1994 and 1997]. KINEROS2 employs a two dimensional linear interpolation scheme to compute model element rainfall intensities from 18 recording rain gages distributed over the intervening area between flumes 2 and 7, and initial soil-moisture conditions, estimated using a continuous soil moisture accounting model run at each of the 18 rain gages (ARDBSN - Stone et al., [1986]). Using observed rainfall and observed inflow at flumes 2 and 7, KINEROS2 was used to compute lateral inflow while adjusting channel infiltration parameters to match observed runoff at flume 1.

In order to calibrate channel loss one must adjust both the rate of infiltration and the area over which infiltration is occurring (i.e. the effective wetted perimeter). The infiltration rate was adjusted by setting K_s for the channel to 0.203 m/hr, which corresponds to estimates for coarse sand [Rawls et al., 1982]. An empirical expression was used to estimate the effective wetted perimeter because, at low flow rates, the trapezoidal channel simplification would introduce significant error [Unkrich and Osborn, 1987]. This relationship was calibrated to most closely match the observed runoff volumes at flume 1 for those events without lateral inflow and that had observed runoff volumes of greater than $\sim 38,000$ m³. The calibration set consisted of seven events ranging from $\sim 38,000$ m³ to $\sim 366,000$ m³.

3.1.2 Direct precipitation on wetted channels and near-channel vegetation. The average total rainfall for five rain gages adjacent to the channel reach between flumes 2 and 1

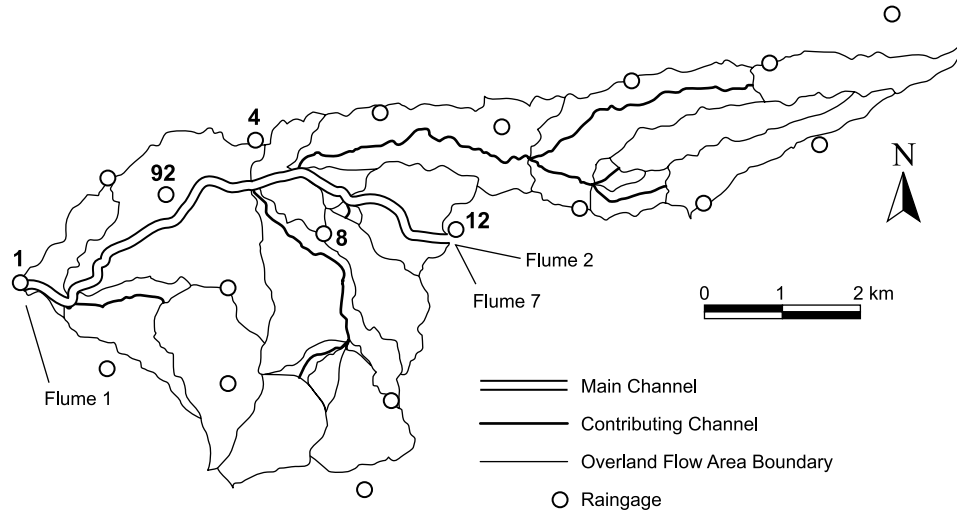


Figure 3. Configuration of watershed elements generated by the AGWA tool and the locations of flumes and raingages. These elements were then abstracted into rectangular overland flow model elements and compound trapezoidal channel elements in KINEROS2.

(raingages 1, 4, 8, 12, and 92 – see Figure 3) were used to compute the direct precipitation on the wetted channel area for each runoff event. This average depth was multiplied by the wetted channel area obtained from the KINEROS2 model runs (see section 3.1.1) to obtain a volume of precipitation for the channel reach water balance.

Due to the change in vegetation density, precipitation on near channel vegetation was estimated for each zone for each rainfall event (see Figure 4). Raingage 12 was used for Zone 1; the average depth of rain from gages 4, 8, and 12 was used for Zone 2 and the average depth of rain from gages 1, 4, and 92 was used for Zone 3. It was assumed that

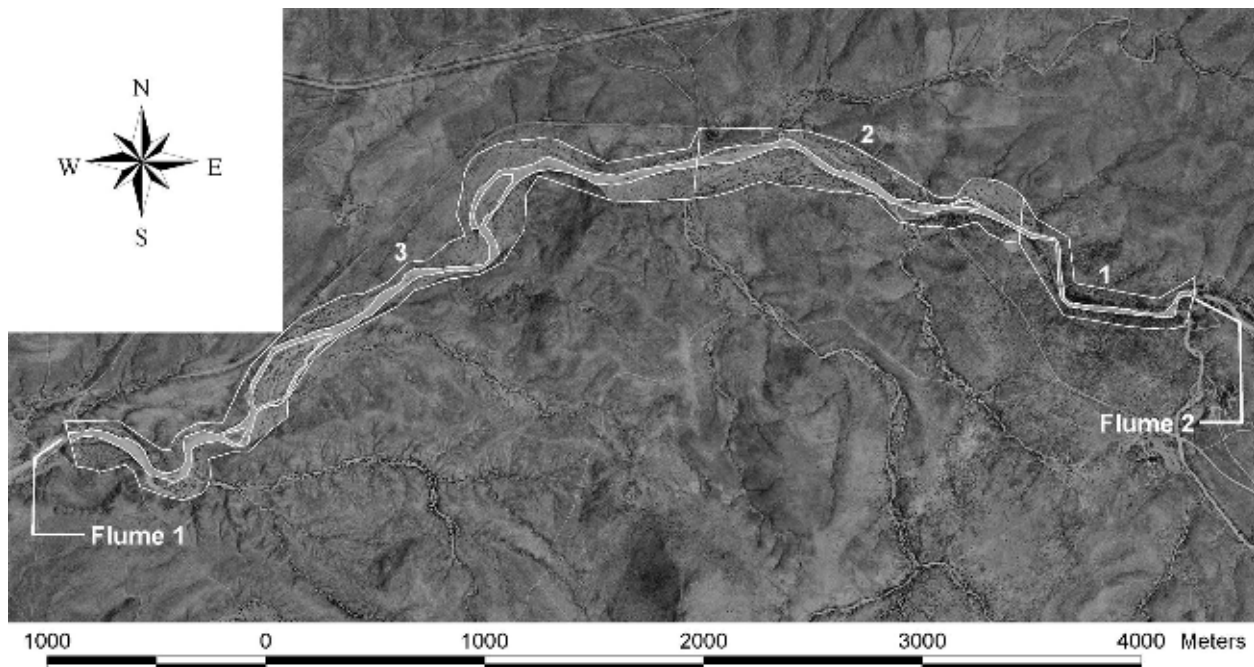


Figure 4. Distribution of the three vegetation zones between Flumes 1 and 2.

precipitation falling on near-channel vegetation less interception (assumed to be 3 mm per event based on measurements by *Tromble*, [1983] for leaf-on conditions and 1 mm per event for leaf-off) would offset plant water use of main channel runoff transmission losses.

3.1.3 Channel evaporation. Total channel evaporation loss for each flow event was computed by multiplying the total wetted perimeter between flumes 1 and 2 from the output of the KINEROS2 model, by the calculated evaporation loss per unit area. Total channel evaporation E_j that occurs from a flow event on day j was calculated using the following formula:

$$E_j = \gamma_n \sum_{i=j}^{j+n-1} PET_i \quad (1 \leq n \leq 15) \quad (2)$$

where n is the number of days between flow events. After 15 days of with no precipitation, evaporation is assumed to be negligible. PET_i was computed with the Penman equation for open water evaporation [*Shuttleworth*, 1993] using data from the Lucky Hills meteorological station. *Sorey and Matlock* [1969] empirically defined γ as the ratio of cumulative evaporation to potential evaporation following a flow event:

$$\gamma_n = \frac{\sum_{i=1}^n E_i}{\sum_{i=1}^n PET_i} \quad (3)$$

where n is again the number of days of drying following a flow event, E_i is the actual evaporation on day i , PET_i is the potential evaporation on day i . Because *Sorey and Matlock* [1969] measured pan evaporation rather than potential evaporation we computed PET_i in Equation 4 by multiplying their pan evaporation totals by a pan coefficient of 0.6.

3.1.4 Near-channel transpiration. Two methods were employed to estimate near-channel tree transpiration. First, sap flow measurements were made on velvet mesquite trees (*Prosopis velutina* Woot.), the dominant near-channel vegetation type, which were then scaled using sapwood to canopy area relationships to estimate channel reach transpiration. Sap flow measurements were made on three mesquite trees at two locations east of flume 2 (Figure 1) in mid-July (early monsoon) and mid-August (mid-monsoon) 1999. Two to four probe sets per tree were inserted at 1.5 m height into exposed sapwood. Every half hour, sap flow was

estimated from the measured heat pulse velocity [*Cohen et al.*, 1981]. Temperature was measured by downstream thermocouples for 60 seconds following an 8-second heat pulse. The time to maximum temperature rise and the maximum temperature difference were used to calculate heat pulse velocity. Corrections were then applied for wounding effects [*Swanson and Whitfield*, 1981, *Burgess et al.*, 2001].

Second, because sap flow techniques are untested on mesquite, we estimated transpiration based on eddy covariance energy balance measurements made at mature mesquite forest adjacent to the main stem of the San Pedro River roughly 10 km southwest of the flume 2 to flume 1 channel reach [*Scott et al.*, 2003]. The mesquites at this site have access to stable regional groundwater and were therefore assumed to provide conservatively high estimates of daily mesquite transpiration. The eddy covariance measurements are detailed in *Scott et al.* [2003].

In order to estimate total canopy transpiration between flumes 1 and 2 transpiration estimates must be scaled to the entire reach length for the full growing season. To scale transpiration to the entire reach we assumed that all vegetation cover was that of mesquite (*P. velutina*). The reach was divided into three vegetation density zones: zone 1 (closest to flume 2) had the greatest cover per unit ground area, followed by zones 2 and 3 respectively (Figure 4). Total sapwood area for each vegetation zone was calculated by determining the relationship between canopy area and basal sapwood area by measuring the basal diameters of seven trees in each zone. Canopy area for each of these trees and the total tree canopy area in the three zones was determined using GIS software and black and white orthophoto maps (Figure 4). Canopy transpiration for the 1999 and 2000 growing seasons was estimated from tree sap flow measured during the 1999 growing season.

Scaling canopy ET to periods when sap flux was not measured requires accurate estimates of the length of the growing season. We estimated growing season length as a function of frost-free days. The timing of spring and fall frost at flume 2 was estimated from temperature data collected continuously at the WGEW Lucky Hills meteorological station. We assumed that nighttime temperatures near flumes 1 and 2 were 5°C cooler than at Lucky Hills. Therefore, temperatures below 5°C at Lucky Hills were assumed to drop below freezing at flumes 1 and 2. The onset of transpiration after the last frost day was estimated from data collected at the San Pedro mesquite eddy covariance site, where the onset of mesquite transpiration began approximately 10 days after the last frost [*Scott et al.*, 2004]. Transpiration was assumed to cease immediately after the first frost at the end of the growing season.

Likewise we used the total canopy area in the three zones to scale eddy covariance estimates of daily transpiration to the channel reach. This was applied for 1999 and 2000 from the first runoff event to the end of the growing season. It was assumed that tree transpiration water use of channel transmission loss water was offset by precipitation less interception. For periods outside the growing season, average winter eddy covariance estimates were used.

3.1.5 Change in storage. The period of the volume balance calculation is from the first runoff event in 1999 to the first runoff event going through both flumes 1 and 2 in 2001. Prior to the first runoff event in each year it is assumed that the state of vadose zone soil moisture in the flume 2 to flume 1 reach to the near channel vegetation rooting depth is at the permanent wilting point. This is a reasonable assumption as an extended dry (typically greater than four months) with high temperatures and low humidity occurs before the monsoon season and the onset of significant runoff generation. Therefore the change in storage is assumed to be zero.

3.2. Groundwater Mounding Model

Channel recharge can be estimated using the groundwater mound equation [Hantush, 1967] which is the solution to a second-order, linear partial differential equation describing an interval of constant recharge rate from stream channel represented by a rectangle of channel width and infinite length to an initially level water table. The equation describes a homogeneous, isotropic unconfined aquifer, and includes the Dupuit-Forchheimer assumption of uniform horizontal flow. Decay of the recharge rate can be computed by superposing the solution for an equal but negative recharge rate, beginning when recharge ceases. One can extend the principle of superposition to approximate a time-varying recharge rate by superposing a series of solutions for incremental negative rates thus allowing the recharge rate to decay exponentially rather than end abruptly from an initially constant rate. This represents the gradual dewatering of the material above the aquifer after a recharge season. At some time all material above the water table becomes unsaturated and the recharge rate diminishes rapidly. For simplicity, the rate was set to zero at this point.

At WGEW, response to individual runoff events could not be discerned in the water level data from the three observation wells at flume 1 (Figure 5), suggesting that the brief, closely spaced pulses of recharge during the monsoon season could be treated as a net constant rate. With this in mind,

solutions to the groundwater mound equation were calculated by a computer program with a graphical user interface. The user interface provided visual, interactive calibration by plotting calculated water levels over observed water levels in response to a change in any calibration parameter. The set of calibrated parameters included the initial constant recharge rates for each season and the horizontal hydraulic conductivity of the aquifer, all normalized by the specific yield of the aquifer material. Also calibrated were the beginning and ending times of the constant recharge periods, and the decay coefficient and cut-off time for the exponential model. Parameterization was accomplished using the graphical interface to visually best fit the data from a given well. With seven parameters to adjust, identifying a unique parameter set depended on having enough independent relationships between the parameters and various aspects of the water level curves.

A similar analysis was conducted by *Moench and Kisiel* [1970] for two wells adjacent to the Rillito Wash in Tucson, Arizona, by scaling and superposing solutions for the groundwater mound equation for a unit recharge rate. Although their method produced recharge rates directly from water level data, it provided no means of calibrating hydraulic conductivity and specific yield, i.e. those values had to be estimated from pumping tests.

3.3. Microgravity Measurements

Repeat microgravity surveys have been used to monitor changes in subsurface water storage and recharge near ephemeral channels in Arizona [Pool and Eychaner, 1995; Pool and Schmidt, 1997]. The method measures changes in subsurface mass by applying Newton's law of gravitation to variations in the results of repeated gravity surveys of a network of stations. Changes between stations are interpolated from the measured stations and integrated across the area of interest to determine total mass change. Changes in gravity were monitored at flume 1 of WGEW from July 2000 through December 2002 at wells 89, 36, 91, and 73 (Figure 2). Measurements were made using a Lacoste and Romberg Model D relative gravity meter and referenced to a station near Tombstone, Arizona, where the absolute acceleration of gravity was measured periodically. The distribution of the stations at the wells near flume 1 should be sufficient to monitor the storage of infiltrated water in the vadose zone beneath the stream channel, the development of a groundwater mound, and the lateral spread of the mound following drainage of water from the vadose zone. The changing subsurface distribution of water mass was simulated using two-dimensional gravity

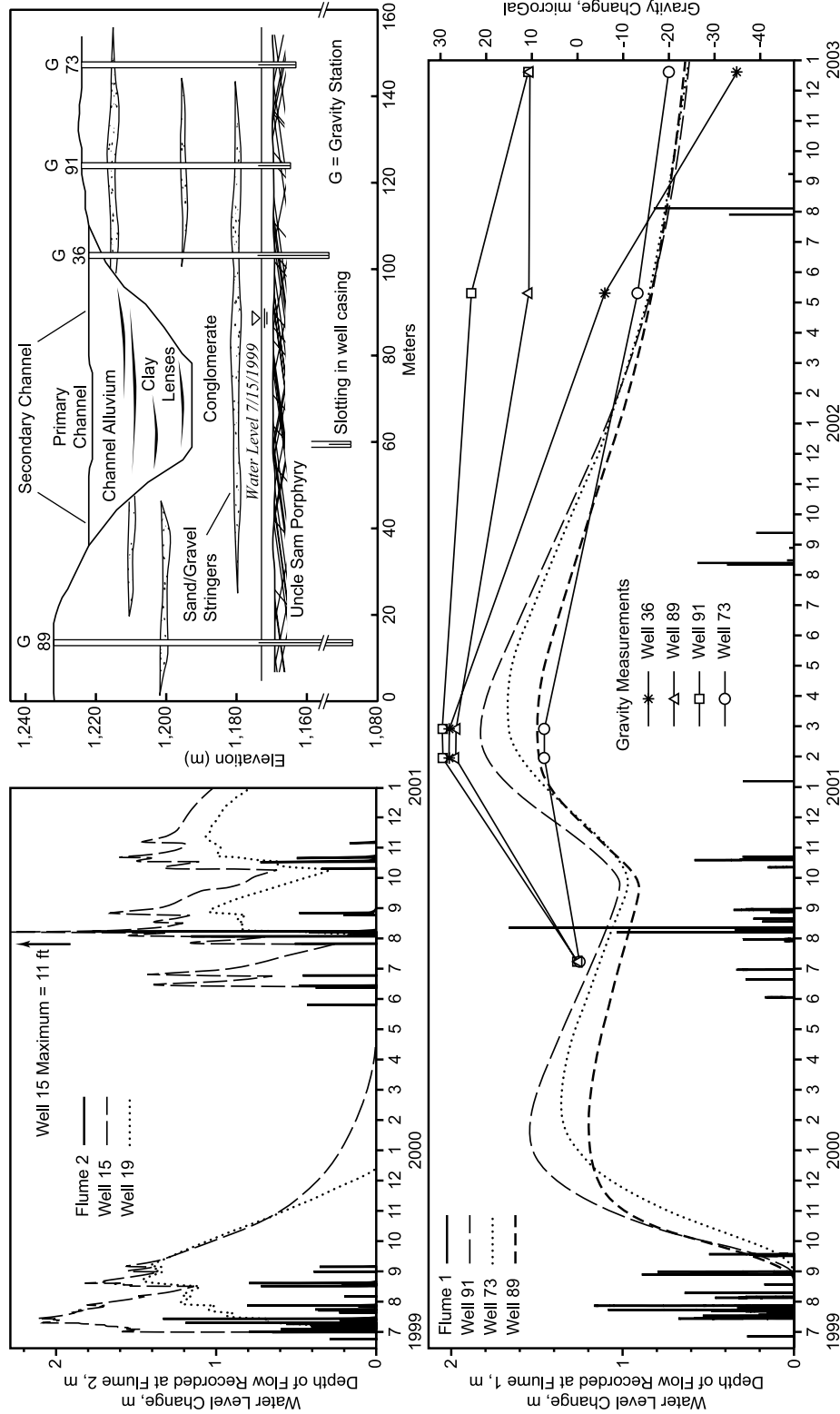


Figure 5. Well levels and flow depths at flume 2 (top) and flume 1 (bottom) and gravity changes at flume 1. Diagram on upper right shows cross section of well transect above flume 1.

models. In order to obtain an overall reach estimate we assumed similar conditions between flumes 1 and 2, based on detailed seismic studies [Libby *et al.*, 1970], and extrapolated the measured storage change at flume 1 along the entire stream reach. The microgravity recharge estimate assumes that steady state or pre-summer 1999 conditions existed during the final survey in December 2002 and the monitoring period was a period of “recovery” from the summer 1999 event with a superimposed summer 2000 event.

3.4. Water Sampling to Determine Chloride Concentration and Stable Isotopes

Stable isotopes of hydrogen and oxygen ($\delta^2\text{H}$, $\delta^{18}\text{O}$) along with Cl and SO_4 concentrations were measured to identify and quantify the source(s) of water to the aquifer near the main Walnut Gulch channel. Isotopic variation is useful for identifying the origin, seasonal timing, and mechanisms of recharge to aquifers in arid and semiarid areas [Allison *et al.*, 1994; Mathieu and Bariac, 1996; Pool and Coes, 1999]. Likewise, because plants do not take up appreciable amounts of Cl and evaporation leaves behind dissolved solids, increased Cl concentrations from rain to runoff to groundwater can be used to estimate the proportion of rain and runoff water which are abstracted from potential recharge due to ET. As applied in this study, this assumes that the observed increase in chloride concentration is the result of near-channel vegetation transpiration and open channel evaporation and that no appreciable groundwater inflow occurs from distant sources that may have different Cl concentrations. The method should only be interpreted as providing a long-term (> one year) integrated estimate of the amount of surface waters abstracted by transpiration and evaporation.

During the monsoon seasons of 1999 and 2000, multiple water samples were collected during runoff events at flume 6 and flume 2. Pump samplers located at both flumes were programmed to begin taking samples when the stage reached one foot. Wells extending to the regional aquifer were sampled before the monsoon to obtain baseline isotope and chloride concentration values. These wells, along with the shallow wells within the perched aquifer, were sampled frequently during 1999, 2000, and early 2001. Replicate samples ($n = 2$ or 3) were averaged to ensure that the water withdrawn was representative of the surrounding aquifer. Rainwater from individual rain events was collected adjacent to both flumes and at the USDA-ARS Tombstone field station located, 5 and 2 km from flumes 2 and 6, respectively. Chloride and sulfate concentrations were determined

on a Dionex DX-500 ion chromatograph equipped with an IonPac PA11 column. Repeated injections of standards determined a precision of 3.5%. $\delta^2\text{H}$ and $\delta^{18}\text{O}$ isotopic values were obtained using a Finnigan Delta S isotope ratio mass spectrometer. Replicate analysis for $\delta^2\text{H}$ agreed within 1‰, whereas $\delta^{18}\text{O}$ values agreed within 0.1‰. In total, more than 300 rain, runoff, and aquifer samples were analyzed in this study. The data presented in this report represents a summary of the most revealing results and trends relating to recharge along this ephemeral channel.

3.5. Vadose Zone Water and Temperature Transport Modeling

Soil-temperature profiles can be used to estimate one-dimensional infiltration fluxes in the vadose zone below ephemeral streambeds [Constantz and Thomas, 1996; Constantz and others, 2003]. Beneath dry streambeds, shallow soil temperatures vary over time in response to the downward conductive heat transport from solar radiation and air temperatures; deeper soil temperatures are not affected by surface temperatures, and therefore do not vary over time. During periods of stream-channel infiltration, heat transport into the subsurface by conduction is considered negligible because advective heat transport by infiltration water dominates subsurface soil temperatures.

During 2001, two vadose-zone boreholes were drilled within the active channel above flumes 1 and 6. Cuttings were analyzed in the field for texture, and the boreholes were logged with an electromagnetic-induction borehole tool to augment the textural analysis. Cores were collected every 1.5 to 3.0 m and analyzed in the laboratory for: pore water tritium activities; thermal properties of specific heat, thermal conductivity, and thermal diffusivity; physical properties of bulk density, porosity, and volumetric water content; and hydraulic properties of saturated-hydraulic conductivity and water retention parameters. Temperature sensors were installed in both boreholes every 1.5 to 3.0 m, from 0 m to a maximum depth of 12.0 m. Soil temperature was then measured and recorded every 30 minutes over a period of about 8 months.

Two approaches were utilized to estimate infiltration flux using heat as a water tracer. An analytical method [Taniguchi and Sharma, 1996; Constantz and Thomas, 1996] was used as a first approximation of infiltration flux from measured soil temperatures at each site. A more comprehensive, rigorous numerical approach was also used, when possible, to account for heat transport with water flow into the vadose zone. The numerical code VS2DH [Healy and Ronan, 1996] was used to simultaneously solve for con-

ductive and advective heat transport with variably saturated water flow. The numerical model simulations were calibrated by adjusting the specified water flux at the upper boundary to minimize the difference between the calculated and measured soil temperatures at depth.

Estimated infiltration rates can then be scaled to calculate the annual infiltration volume (i.e. transmission loss) for the entire length of channel between flumes 2 and 1. This is done by first scaling the infiltration rate to the duration of streamflow to calculate an annual infiltration depth. The annual infiltration volume can then be calculated by applying this infiltration depth to the wetted area of the stream channel. The wetted channel area is estimated using the channel length and the wetted channel width calculated by KINEROS2 (section 3.1.1). Annual channel recharge can then be estimated by subtracting the annual water lost due to open channel evaporation (section 3.1.3) and near channel transpiration (section 3.1.4) from the annual infiltration volume.

RESULTS AND DISCUSSION

Runoff and groundwater levels from the 1999 monsoon seasons through 2002 are presented in Figure 5. In terms of both number and size (total annual volume) of runoff events, the 1999 monsoon season was the largest of the approximately 30 years of observations. Runoff events for the 2000 monsoon season were fewer in number but occurred over a longer period of time than the 1999 monsoon. Of note is the August 11, 2000 event, one of the largest recorded, and a series of four events in late October that occurred after the typical mid-September end of the monsoon. In contrast, runoff for the 2001 monsoon season totaled only 43,000 m³ at flume 1 compared to 1.77 million m³ in 1999 and 1.04 million m³ in 2000.

Significant groundwater level response was observed in both the shallow and deep wells (Figure 5). Shallow wells above flume 2 were nearly dry before the start of the monsoon season. These wells responded rapidly to runoff events, with the most rapid response occurring in the well closest to the channel (well 15) and increasing in response time with greater distance from the channel. In contrast the deep wells responded roughly a month after the onset of significant monsoon runoff events with water levels continuing to increase for roughly six months. No increase in deep groundwater level was observed after the 2001 monsoon season even though some runoff and infiltration did occur thus indicating that some threshold volume of stream channel infiltration must be overcome before deep aquifer recharge can occur.

4.1. Channel Reach Water Balance

The components of the channel reach water balance for the 1999 and 2000 monsoon seasons are summarized in Table 1. In the following explanation of results, separate subsections are not included for individual water balance components, such as open channel evaporation, channel precipitation, and precipitation on near-channel canopy less interception, that are obtained by straight forward calculations. Subsections are included where comments on the results are warranted. This is followed by an evaluation of the overall reach water balance.

4.1.1. Channel transmission losses. KINEROS2 simulations indicated that 27 of the 48 flow events that occurred in 1999 and 2000 produced lateral inflow. After calibration of the effective wetted perimeter equation, the modeled runoff volume at flume 1 was within 2.5% of the total observed runoff volume for 1999 and 2000. This is comparable to the measurement accuracy of the Walnut Gulch supercritical flumes used to measure the runoff [Smith *et al.*, 1982]. The Nash-Sutcliffe statistic for all 48 runoff events was 0.97, indicating the model predicted observed runoff with a high degree of accuracy (if perfect the Nash-Sutcliffe statistic would equal one). Table 1 presents transmission loss as a range of values for each year reflecting the error associated with simulating the lateral inflow and an error associated with routing flow through the main channel stem (Table 1, shown in parenthesis). These two sources of error were considered to be random, independent, and additive.

4.1.2. Near-channel tree transpiration. Daily sap velocities were 94 cm/day for July (SE = 8.0, n = 5 days), 121 cm/day in August (SE = 2.0, n = 5), and 79 cm/day in October (SE = 3.5, n = 5 days). Sap flow rates exhibited no correlation with changing groundwater depth or monsoon runoff events. These data suggest that during monsoon periods when water is not limiting, climatic drivers, such as photosynthetically active radiation (PAR) and leaf to air vapor pressure deficit are the primary factors that control transpiration [Cienciala *et al.*, 2000]. Sap flow estimates of mesquite transpiration were scaled to the tree canopy level and finally to daily transpiration depth per unit area (~0.3 mm/day). The resulting transpiration rates were significantly lower than anticipated and were closer to bare soil or winter rates. Estimates an adjacent mesquite site on the San Pedro River (~4.3 mm/day) and the Santa Cruz riparian area (~4.1 mm/day) [Scott *et al.*, 2003; Unland *et al.*, 1998]. It was judged that the sapflux derived values of mesquite transpiration were far too low to be realistic and were there-

Table 1. Summary of water mass balance between flumes 1 and 2&7 for 1999-00 and 2000-01 to nearest 1000 (m³).

Inputs	1999-2000 (m ³)	2000-2001 (m ³)
Flume 1 (measured)	1,778,000	1,048,000
Flume 2 (measured)	1,763,000	1,326,000
Flume 7 (measured)	248,000	49,000
Modeled Lateral inflow	281,000 (77,000)	102,000 (72,000)
Modeled Trans. Losses	437,000 – 591,000	358,000 – 501,000
<u>Terms of Reach Water Balance (Eq. 1)</u>		
Midpoint Modeled Trans. Losses	514,000	429,000
Precipitation on Wetted Channel	9,000	6,000
Precipitation on Canopy - Interception	27,000	39,000
<i>Total Inputs</i>	<u>550,000</u>	<u>474,000</u>
Abstractions		
Channel Evaporation	1,000	1,000
Near Channel Transpiration (Energy/Flux Est.)	77,000	103,000
<i>Total Abstractions</i>	<u>78,000</u>	<u>104,000</u>
Total Potential Recharge	472,000	370,000

fore not used in the water balance summarized in Table 1. Further investigation indicated that the active sapwood area of mesquites is highly irregular and relatively thin as compared to the sap flux heat source and thermal sensor probes. Further research is being done to determine if this type of sap flux sensing method is appropriate or can be modified for mesquite trees.

In lieu of the sap flux based estimates of mesquite transpiration, the average daily eddy correlation-based estimates of transpiration (4.3 mm/day) from the nearby well watered mesquite forest were used [Scott *et al.*, 2003]. There were 85 and 134 days from the first runoff event to the end of the growing season in 1999 and 2000, respectively. In the non-growing season a conservatively high average ET rate of 0.25 mm/day was used. Total canopy area in the near channel zone was estimated to be ~103,000 m² (~10% canopy cover, Figure 4). These data were used to scale the daily transpiration rate to provide estimates for the entire 1999 and 2000 runoff seasons between flumes 2 and 1. Transpiration water use of runoff transmission loss waters was then reduced by precipitation less interception falling on the canopy noted as an abstraction in Table 1. This assumed that the extent of lateral surface roots roughly corresponded to the canopy area.

4.1.3 Recharge estimates from channel reach water balance. Because the KINEROS2 model accounts for measured runoff injected into the upper end of the reach from flumes 2 and 7, computes lateral inflow, and attempts to match measured runoff at flume 1, Equation 1 is effectively reduced to:

$$R = TL_{MOD} + P - T - E \quad (4)$$

In Equation 4 the KINEROS2 modeled transmission losses (TL_{MOD}) are supplemented by precipitation on the runoff wetted area of the channel (P) and reduced by the abstractions of evaporation from the wetted channel (E) and near-channel transpiration adjusted for precipitation less interception on the canopy (T).

For the relatively wet runoff years of 1999-00 and 2000-01, the estimated potential recharge from the reach water balance was 472,000 and 370,000 m³, respectively. Computed transmission losses greatly dominated the overall estimation of potential recharge as total abstractions, as a percentage of total inputs, were only 14% and 22% respectively, for 1999-00 and 2000-01. Because the abstractions are largely dependent on the quantity of rainfall and runoff, it is expected that during dryer years, the percentage of overall abstractions would not increase greatly.

4.2. Recharge Estimates From Groundwater Mounding Model

The groundwater mounding model was only applied to observations from wells 89 and 91. Well 73 was not analyzed because the geochemistry results (section 4.4) indicated that they were not receiving direct recharge from the stream channel. The Hantush equation was able to closely reproduce the observed well level data over the first 300 days of each season (Figure 6), but was not successful in fitting the final slope of the water level recessions. The observed data indicated a nearly constant final recession

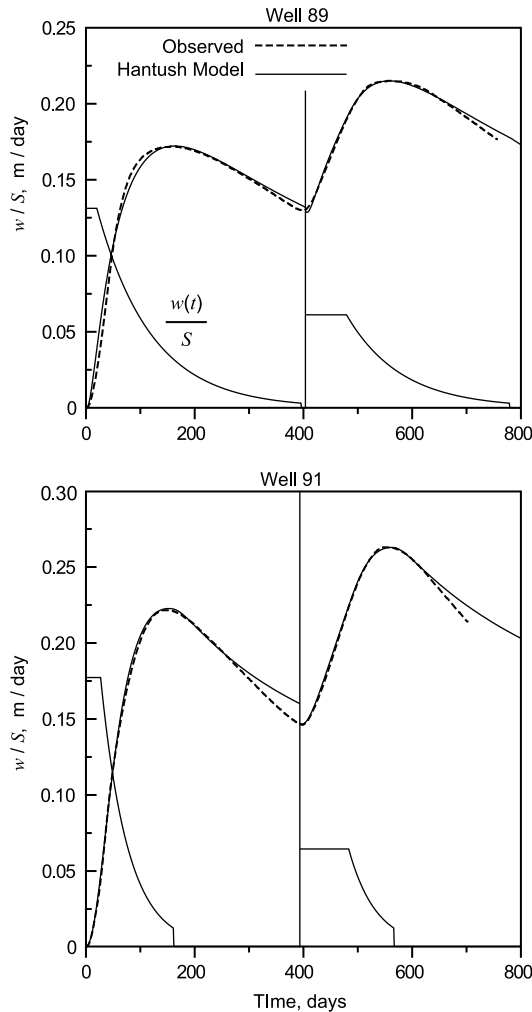


Figure 6. Results of fitting the Hantush groundwater mound equation to data from the three observation wells. $w(t)$ is the time-varying recharge rate, S is the specific yield, h is the water table depth, and h_0 is the initial depth.

rate, whereas the Hantush equation produced an exponential rate. Note that the hydraulic conductivity and specific yield were held constant over the two recharge periods, as there was no information available on cyclic or long-term temporal changes.

Calibration of the Hantush equation appeared to produce a definite, unique relationship between equation parameters and characteristics of the water level curves. For example, matching the well-level rise rate dictated a specific combination of initial recharge rates and hydraulic conductivity. Ideally, for an isotropic and homogeneous aquifer, the parameter sets for each well would be the same, however each dictated a unique parameter set (Table 2). To calculate

recharge rates we must therefore assume that each well represents an independent aquifer of sufficient extent and uniformity for Dupuit-Forchheimer flow to apply and that each well may receive a different amount of recharge. This could be caused by interception and diversion of infiltrating water by clay lenses in the channel alluvium.

Total recharge volumes for each season per unit area of channel were computed by integrating the recharge rate curves for each season and multiplying the result by specific yield. Specific yield was calculated for conglomerate and unconsolidated material, using densities values for these materials measured by *Wallace and Spangler* [1970] and assuming a density of 2.67 gm/cm³ for solid material; these values were used to calculate high and low recharge estimates (Table 2). Recharge rates were then multiplied by the inundated channel area from the KINEROS2 simulations, in order to calculate total recharge volumes (Table 2).

4.3. Recharge Estimates Based on Microgravity Changes

Gravity changes during the July to December 2002 monitoring period (Figure 5 - lower panel), exhibited two distinct periods of change that generally correlated with water levels. The first was a period of increasing gravity that occurred from July 2000 through January 2001 and was related to streamflow events and drainage of water that infiltrated during 1999 and 2000. The second was an extended period of decreasing gravity from February 2001 through December 2002 when streamflow and infiltration was minimal.

During the first period, gravity values for wells closest to the channel (89, 36 and 91) increased by 26 to 29 microGal, whereas values for the well farthest from the stream channel increased by only 8 microGal. Coincident with the gravity increase was a water-level rise of roughly 1m at each well. Water levels were not measured at well 36 because the casing had previously filled with sand. In an unconfined aquifer, with a specific yield of 0.20, a laterally extensive 1m change in water level would result in a gravity change of about 8 microGal. Based on this, the gravity increase at well 73 can likely be explained by the 1m water level rise. In contrast, gravity changes for wells located closer to the stream channel were greater than those for a 1m change in groundwater level, indicating an increase in vadose zone water storage. Gravity decline during the second period was greatest closest to the channel, with well 36 decreasing by 63 microGal whereas further from the stream channel gravity decreases were less (19, 16 and 28 microGal at wells 91, 89, and 73, respectively). At the same time water levels declined by roughly 1 m, indicating that vadose zone water

Table 2. Fitted parameter values and recharge estimates from groundwater mounding model. High and low estimates were obtained using the porosities of the conglomerate (0.124), and unconsolidated material (0.243) to the nearest 1000 m³.

Well	Fitted Parameters				Recharge Volume (m ³)					
	Initial Recharge Rate (m/day)		Hydraulic Conductivity (m/day)	Decay Coeff	1999–2000			2000–2001		
	1999	2000			Low	High	Average	Low	High	Average
89	0.024	0.012	2.15	0.01	127,000	250,000	188,000	86,000	169,000	127,000
91	0.033	0.012	0.74	0.02	107,000	211,000	159,000	69,000	135,000	102,000

storage also decreased during the period. Finally, during the second period gravity decline at well 73 was in excess of that required by the water-level decline and thus must be due to some vadose zone storage loss. The lateral extent of this loss is difficult to assess because there are no gravity stations beyond well 73 but it is likely a local phenomenon related to heterogeneities near flume 1 (an abandoned stream channel). These heterogeneities likely do not occur elsewhere along the reach and because of this the gravity data from this well was not included in the evaluation of recharge rates.

The distribution of storage loss for the second period was simulated with a two-dimensional gravity model. Storage change in the unconfined aquifer was constrained by the water-level change and a specific yield of 0.20. The remainder of the storage change was distributed in the vadose zone to match the observed gravity change. The resulting model was sufficient to explain the gravity decrease at wells 36, 89 and 91 and indicated that nearly all observed storage loss occurred directly beneath the stream channel, most likely as the result of water drainage from the vadose zone to the saturated groundwater system. The simulated vadose zone storage loss required a 10 percent change in volumetric water content, a reasonable change for the highly porous sand and gravel deposits. Variation in the simulated vadose zone water content would primarily result in variations in the width of the region of storage change, but little variation in the general location of the storage change. Other changes in water content could also explain the gravity change; however, the general model results are well constrained by the observed data.

Finally, during the second period, gravity decline at well 73 was in excess of that required by the water-level decline and thus must be due to some vadose zone storage loss of undetermined lateral extent. The occurrence of vadose zone water at well 73 is likely a local phenomenon related to local heterogeneities near flume 1 that do not likely occur elsewhere along the reach. As noted in the following section, there is evidence to suggest that a substantial portion of the water in well 73 has an origin *other than ephemeral*

channel runoff. Delayed recharge of the aquifer near well 73 by deep percolation of vadose zone water may help explain the high recharge rate determined from the groundwater mound analysis.

4.4. Geochemical Tracers

4.4.1 Oxygen and hydrogen isotopes. Tracing the pathways and timing of recharge with stable isotopes is possible if there is a significant difference in the isotopic signatures of runoff and groundwater. Differences may arise from variations in water source (timing of recharge or change in recharge location) or result from evaporation prior to recharge. The relationship between hydrogen and oxygen isotope composition of precipitation, runoff, and deep groundwater for 1999 has a slope of 7.9, close to that of global precipitation ($s = 8.1$, Rozanski *et al.*, [1993]) indicating little or no evaporative enrichment (Figure 7). Different water sources exhibited distinct patterns of isotopic composition. Deep groundwater wells had a relatively uniform isotopic composition typical of the regional aquifer on the east side of the basin [Pool and Coes, 1999]. In contrast, precipitation and runoff isotopic compositions were highly variable and both heavier and lighter than deep groundwater. $\delta^2\text{H}$ and $\delta^{18}\text{O}$ values for individual runoff events closely tracked that of the precipitation (Figure 8). Variation within individual events was small; $\delta^2\text{H}$ values typically increased between 4 and 10 ‰. However, the storm-to-storm variation was quite large and included an anomalous period of isotopically light precipitation from July 19 to July 29, 1999 (DOY 200–210). Typically, summer rainfall in the American Southwest is enriched in $\delta^2\text{H}$ and $\delta^{18}\text{O}$, however the isotopic composition of rainfall during early monsoon period in 1999 was more like that of winter-time precipitation [Wright, 2001]. During the 2000 monsoon season, $\delta^2\text{H}$ values of runoff ranged from –53 to –40 ‰, isotopically similar to that of the deep aquifer, and thus were not as useful for tracing recharge.

The lack of a distinct isotopic signal for runoff limits our ability to quantify the amount of ephemeral channel

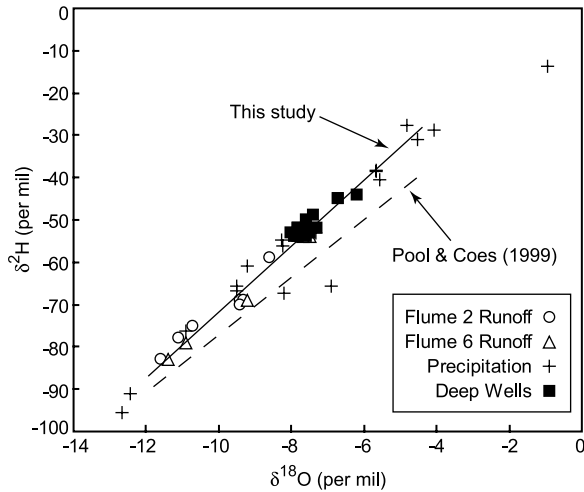


Figure 7. Relation between the hydrogen and oxygen isotope composition of precipitation, runoff, and deep groundwater collected in 1999 from Walnut Gulch. Regression line ($\delta D = 7.9 * [\delta^{18}O] + 7.1$; $r^2 = 0.97$) from current study is from runoff and deep aquifer samples only. Regression line ($\delta D = 7.0 * [\delta^{18}O] - 4.6$; $r^2 = 0.92$) calculated from *Pool and Coes* [1999] is from runoff and aquifer samples collected across the whole upper San Pedro watershed area, including samples from the alluvial aquifer of the San Pedro River.

recharge. However, two large runoff events during the period of isotopically light precipitation were sufficiently distinct from deep groundwater (-11.6 and -9.3 ‰ for $\delta^{18}O$, -83 and -69 ‰ for δ^2H) to allow a qualitative assessment of the timing and spatial pattern of recharge within WGEW. Prior to the onset of the 1999 monsoon runoff, $\delta^{18}O$ values of the deep groundwater ranged from -7.8 to -6.7 ‰ and δ^2H values ranged from -54 to -45 ‰. Of the 13 deep wells sampled in this study, 11 wells showed virtually no change in isotopic composition over the two years of sampling, while two shifted to more negative δ^2H and $\delta^{18}O$ values in response to the isotopically depleted runoff events in 1999 (Figure 9). These wells, located between flumes 2 and 1 on the lower end of the watershed, had the heaviest isotopic composition prior to the start of the monsoon. Well levels continued to increase in response to the 2000 monsoon events, but isotope samples collected in February 2001 (data not shown) revealed no change from December 2000 values, likely reflecting the lack of isotopic variation between 2000 monsoon runoff water and that of the deep aquifer.

Isotopic analysis results provide a conceptual model of ephemeral channel recharge at WGEW that is dominated by relatively rapid transmission through very porous alluvium precluding significant opportunity for evaporation in the unsaturated zone [Dincer et al., 1974]. The relatively small

percentage of evaporation and transpiration abstractions from ephemeral channel transmission losses supports this conclusion (see section 4.1.3 and Table 1). The lack of isotopic variation for an individual event suggests that the storm generating the runoff was isotopically homogeneous, or the runoff integrated the spatial or temporal isotopic variation in the rainfall. Evidently, direct and fairly rapid recharge to the deep aquifer is taking place within the very dynamic zone in the lower sections of Walnut Gulch.

4.4.2. Recharge estimates from chloride concentrations in runoff and well water.

Chloride mass balance has long been

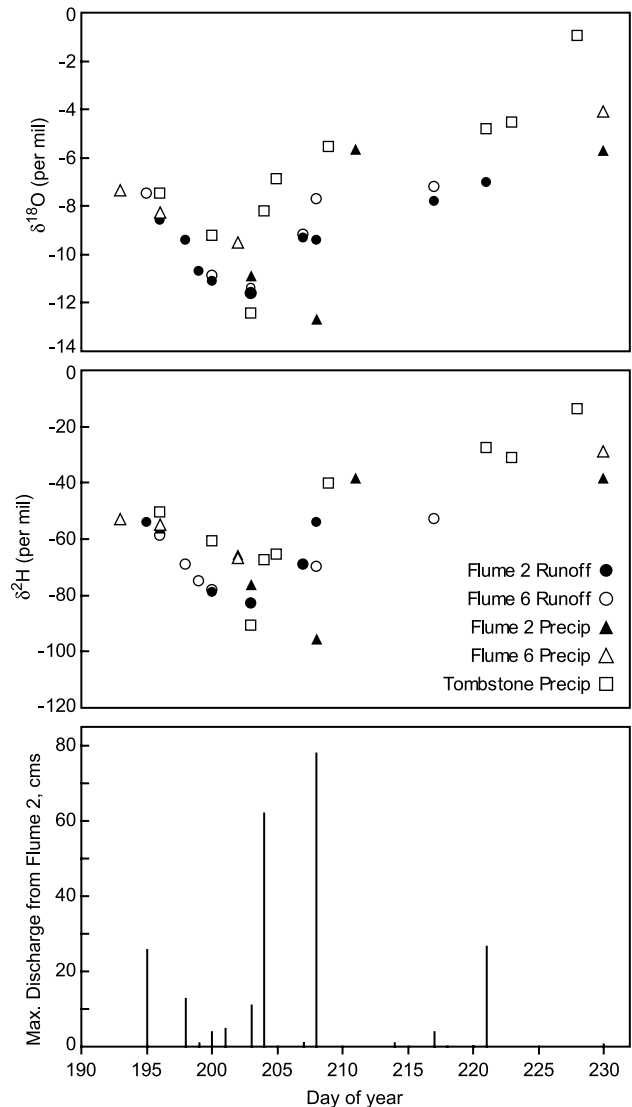


Figure 8. Oxygen and hydrogen isotope composition of rainfall and runoff during 1999, and maximum discharge rates at flume 2.

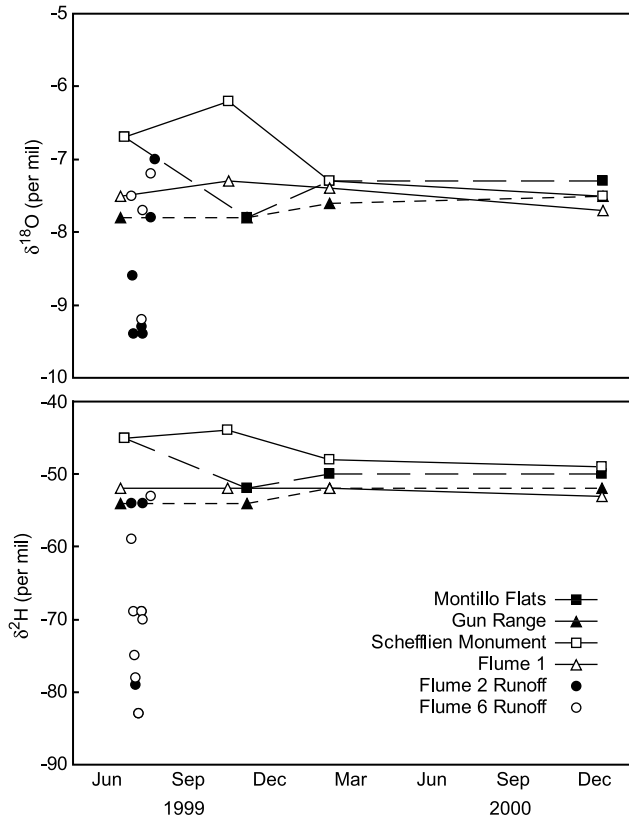


Figure 9. Oxygen and hydrogen composition of deep wells and runoff. Wells presented include two isotopically dynamic wells (Montillo Flat and Schefflien Monument) and two wells that exhibited no change (Gun Range and Flume 1 channel wells).

used to estimate recharge rates through desert vadose zones [Scanlon, 1991; Allison *et al.*, 1994; Phillips, 1994; Wood *et al.*, 1997] to quantify an average regional recharge flux to a large aquifer systems [Eriksson and Khunaksem, 1969; Dettinger, 1989; Wood and Sanford, 1995], and even to determine riparian evapotranspiration losses [Gatewood *et al.*, 1950]. For this study we modified this approach to quantify ephemeral channel recharge by examining the increase in chloride concentration from precipitation to runoff to groundwater. One potential complication with this approach is distinguishing groundwater derived from ephemeral channel recharge and regional groundwater that likely has higher chloride concentrations. We use $[SO_4]/[Cl]$ ratios, which are not affected by evapotranspiration, to distinguish between these waters and their mixtures.

The chloride concentration of precipitation collected at flumes 2 and 6 averaged 0.31 ± 0.07 (1SD) ppm; sulfate concentrations were not measured. Runoff events were sampled at flume 2 and flume 6 during 1999 and 2000.

Sampling problems during 1999 (water fouling, sediment clogging, etc.) affected these samples, which are not included in this analysis. Runoff samples from 2000 exhibit significant variation in Cl concentration and $[SO_4]/[Cl]$ ratios with no discernable trend in time or space (Figure 10). In an attempt to obtain representative Cl concentrations and $[SO_4]/[Cl]$ ratios, we calculated volume-weighted averages for each storm event at each flume. Volume weighting was done only for those intervals when samples were collected, using a linear interpolation for [Cl] and $[SO_4]$ concentration between samples (~20 min). The resulting Cl concentration (0.62 ± 0.34 ppm) and $[SO_4]/[Cl]$ ratio (17.2 ± 16.6) were assumed to be the average for both runoff waters and channel transmission losses. In comparison, regional groundwater has higher Cl concentration and lower $[SO_4]/[Cl]$ ratios (Figure 11). Wallace and Cooper [1970] noted high Cl concentrations (up to 40 ppm) in groundwaters from the regional aquifer, the source of which appear related to large granitic intrusions in the Tombstone Hills. Well water collected near the stream channel exhibits values intermediate between these two end-members: well 73 exhibits elevated Cl concentrations and lower $[SO_4]/[Cl]$ ratios, indicating mixing of ephemeral channel recharge with regional groundwater, whereas well 89 exhibits only increased chloride concentration, indicating evapotranspirative loss prior to recharge, with no mixing with regional groundwater. Well 91 waters were similar to those of well 89 (Cl concentration of 1.13 ppm in well 91 versus an average of 1.09 in Well 89), but this was based on a single sample from well 91.

Ephemeral channel recharge volumes may be calculated in two ways. The first approach is the most straight-forward, given the available observations. It utilizes the increase in Cl concentration from runoff (0.62 ppm) to groundwater (1.09 ppm) to determine that 57% of transmission losses result in groundwater recharge, with the rest lost as near-channel evapotranspiration. Using midpoint-modeled transmission losses (Table 1) of 472,000 m³ for 1999-00 and 370,000 m³ for 2000-01 results in groundwater recharge volumes of 269,000 and 211,000 for the channel reach between flumes 2 and 1.

The second approach assumes more commonly available information that could be applied more readily over large regions where detailed data associated with the experimental watersheds are not available (i.e., almost everywhere). Let us assume Cl concentrations are available from local precipitation and that one or more near channel wells are available along with some knowledge of local hydrology (hillslope runoff ratios), total basin outflow (e.g. a USGS gage), and total precipitation over the basin (e.g., rain gages

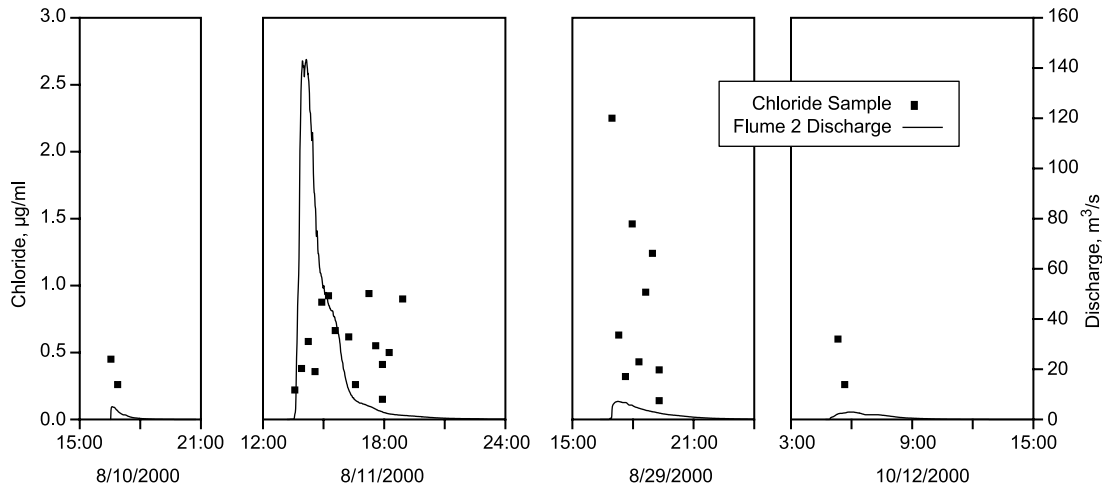


Figure 10. Discharge rate and Cl concentration at flume 2 in 2000.

or radar-rainfall estimates). From the data collected in this study, the increase in Cl concentration from 0.31 ppm in precipitation to 1.09 in groundwater would indicate that 28% of the precipitation that produces runoff results in groundwater recharge. Longer-term water balance observations at the WGEW indicate that the hillslope runoff ratio is ~7% of precipitation, whereas the remaining precipitation results in surface detention and infiltration [Renard *et al.*, 1993]. In desert regions, essentially all hillslope infiltration returns to the atmosphere, storing the associated Cl in the vadose zone [Phillips, 1994; Walvoord, 2002; Walvoord *et al.*, 2002; Scanlon *et al.* 2003]; thus, this Cl can be removed from mass balance considerations. Of the 7% of precipitation that results in hillslope runoff, ~9% leaves the overall watershed outlet (flume 1) as runoff and must also be removed from the mass balance calculation. The resulting watershed runoff ratio for all of the WGEW is ~0.6%. Using the densely gauged WGEW (Figure 1), an annual precipitation volume of 49 million m³ in 1999 and 63 million m³ in 2000 was estimated. The 7% runoff ratio less the 9% of that runoff that exits the watershed results in a channel loss volume of 3.1 million m³ in 1999 and 4.0 million m³ in 2000. Using the 29% recharge ratio, the calculated recharge volume is 0.9 million m³ and 1.2 million m³. Note that this recharge volume is for the entire channel network of WGEW, assuming no recharge from hillslope areas. To downscale to the reach between flumes 2 and 7 and flume 1 we can apply the ratio of the area of all channels contributing to this reach to the area of all channels in the watershed (0.21) as digitized from high-resolution orthophoto maps [Goodrich *et al.*, 1997]. Applying this ratio, a scaled potential recharge of 189,000 and 252,000 m³ in 1999 and 2000,

respectively, is estimated. A more readily available scaling ratio is simply the ratio of drainage areas between the flumes 2 and 7 to flume 1 reach to the total watershed area (0.15). Using this ratio, a scaled potential recharge of 135,000 in 1999 and 180,000 m³ and 2000 is estimated.

4.5. Vadose Zone Water and Temperature Transport Modeling

Stream channel sediments from the borehole located just upstream of flume 1 consist of sand and gravel stream alluvium in the upper 14.5 m, underlain by basin fill that

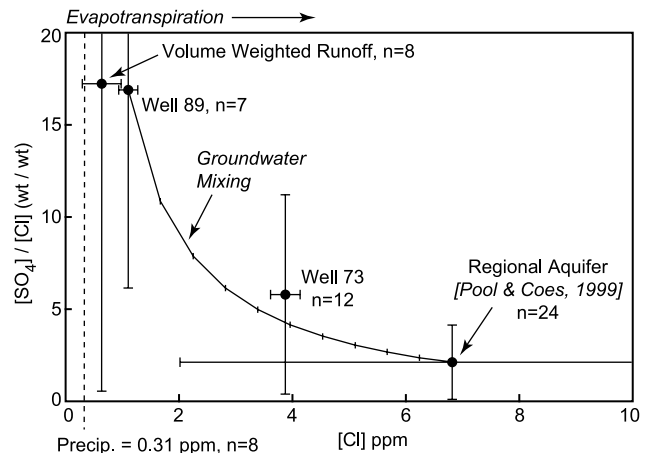


Figure 11. Precipitation, runoff and groundwaters at WGEW plotted on a $[SO_4]/[Cl]$ vs. $[Cl]$ mixing plot. Error bars represent 1 SD for averaged values. Also plotted is a mixing trend, in 10% increments, between regional groundwater and “ephemeral channel recharge” groundwater (Well 89).

includes 20- to 55-percent silt and clay. Sediments from the second borehole located just upstream of flume 6 consist of unconsolidated sand and gravel stream alluvium to 3.7 m, consolidated conglomerate of lower basin fill from 3.7 to 11.6 m, and basalt from 11.6 to 12.2 m. Laboratory measurements of core samples from the flume 1 site indicate little variation between the stream alluvium and the upper basin fill. The measured saturated hydraulic conductivity of the cores ranged from 0.02 to 0.046 cm/s; porosity ranged from 0.35 to 0.47; and, water content ranged from 0.10 to 0.25. Hydraulic and physical properties were not determined for the stream alluvium or the lower basin fill at the flume 6 site. Pore water tritium activities to 22.4 m at the flume 1 site, and to 2.3 m at the flume 6 site, were comparable to present-day precipitation, indicating that recent infiltration has occurred to at least these depths at both sites.

During the April to December 2002 monitoring period, three ephemeral flow events occurred at flume 1, and seven occurred at flume 6. At flume 1, temperature perturbations were detected during and/or after each event at 1.5, 3.0, 4.6, and 6.1 m; but no temperature perturbations were detected below 6.1 m. Calculated infiltration fluxes to 4.6 m during the flow events ranged from 0.012 to 0.058 cm/s, whereas infiltration fluxes immediately after the flow events ranged from 0.0038 to 0.029 cm/s (Figure 12). While seven events occurred at flume 6, only soil temperatures from the July 19, 2002 flow event could be used at this site because the borehole was damaged some time after mid-July 2002. During this event, a temperature perturbation was detected at 3.0 m. The infiltration flux to 3.0 m during this flow event ranged from 0.010 to 0.029 cm/s.

Estimates of the annual recharge along the length of Walnut Gulch from flume 2 to flume 1 were based on the above-calculated infiltration fluxes. The lowest calculated infiltration flux for the period of time after flow events (0.0038 cm/s) can be scaled using flow durations from runoff measurements at flumes 1 and 2 and the average annual wetted channel width, determined to be 15-percent of the alluvial channel width obtained from 1988 orthophotography. Average annual wetted channel widths were derived from KINEROS2 output of the maximum wetted area for each event (see sections 3.1.1 and 4.1.1 for more details). The resulting channel transmission losses were adjusted for channel evaporation (1,000 m³/yr for 1999-00 and 2000-01) and near-channel transpiration (77,000 and 103,000 m³/yr for 1999-00 and 2000-01, respectively; Table 1). Total annual recharge through the streambed between flumes 1 and 2 was 438,000 m³ in 1999 and 163,000 m³ in 2000.

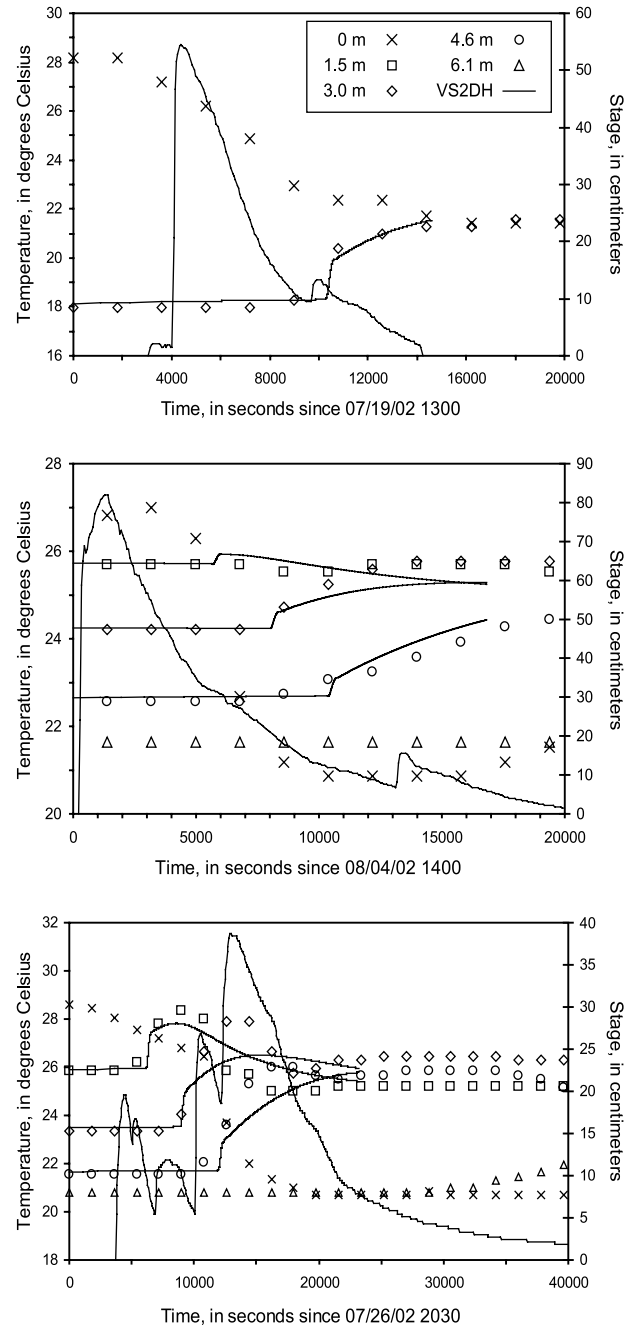


Figure 12. Thermographs of observed data and VS2DH model output for borehole sites at: a) flume 1 on July 26, 2002; b) flume 1 on August 4, 2002; c) flume 2 on July 19, 2002.

4.6 Comparison of Methods

This study provides a unique opportunity to compare three distinct types of methods for estimating ephemeral

Table 3. Comparison of recharge estimates for all methods, flume 2 to flume 1. All values are in cubic meters and are rounded to the nearest 1000 m³.

Year	Water Balance		Change in Water Volume		Tracers		
	Reach Water Balance	Simplified Reach Water Balance ^a	GW Mound Model (Well 89)	Micro-gravity	Cl Mass Balance	Simple Cl Mass Balance ^b	Vadose Zone Temperature Modeling
1999-00	472,000	233,000	188,000		269,000	135,000	438,000
2000-01	370,000	327,000	127,000		211,000	180,000	163,000
'99-'00 Total	842,000	560,000	315,000	455,000	480,000	315,000	601,000

^aReach inputs measured at Flumes 2 and 7 minus reach output at Flume 1

^bUsing precipitation to well water Cl concentration ratio, local runoff ratios, and drainage area scaling (see section 4.4.2)

channel recharge: reach water balance; geochemical and geophysical tracers; and direct and indirect measurements of water volume change. In comparing these methods, we will first evaluate recharge estimates, the size and source of errors related to each method and why certain methods may be biased high or low. We will then discuss the lessons learned and general applicability of each method by considering the ease of use, major pitfalls, data requirements, and the spatial and temporal scaling necessary.

Estimated recharge volumes from all the methods are within a factor of three (Table 3). The general agreement is encouraging and indicates that each method is capable of estimating ephemeral channel recharge on a yearly basis at

the channel reach scale. This level of agreement is impressive given the high degree of uncertainties in key parameters for each method (Table 4). As noted earlier, a full error analysis is beyond the scope of the paper. Furthermore, the limited data collection would not provide an accurate representation of level of error that could be achieved for each method. A few examples, drawn from the three types of methods, should however illustrate the degree of uncertainty introduced in each method.

In the case of the reach water balance the source of greatest uncertainty is related to estimating lateral channel inflows. An error analysis (not included here) was conducted to estimate the magnitude of error in estimated lateral

Table 4. Relative merits and weaknesses of recharge methods employed in this study.

	Water Balance		Change in Water Volume		Tracers		
	Reach Water Balance	Simplified Reach Water Balance	GW Mound Model (Well 89)	Micro-gravity	Cl Mass Balance	Simple Cl Miss Balance	Vadose Zone Temperature Modeling
Requirements	Extensive instrumentation	Accurate discharge measurements in alluvial channels	Near-stream well levels	Periodic surveys using a gravity meter	Cl in runoff and wells, channel infiltration volumes	Cl in precipitation and wells, basin precipitation, and local runoff ratios	Unsaturated zone properties, unsaturated soil temps with depth, flow duration, channel wetted area
<i>Most Uncertain Aspect</i>	Lateral inflow	Runoff measurements	Aquifer conductivity and specific yield	Spatial and temporal distribution of data	Is GW Cl strictly from runoff recharge	Basin-wide precipitation	Channel wetted area
<i>Scaling to Reach from</i>	–	–	Well Point	Channel Cross Section	Well Point	Drainage Areas	Borehole

inflow (shown in parentheses in Table 1). These errors can be large, over 25% and 70% respectively, in 1999–00 and 2000–01. At the high end, modeled lateral inflow was only 18% and 13% of the reach inflow (flume 2 plus flume 7) for these two time periods, however these values are roughly three-fourths and one-half the size of the calculated transmission losses. For chloride mass balance, the variability in the Cl concentration of ephemeral flow and groundwater (1SD) yields recharge fractions that range from ~20% to greater than 100%. Finally, for the temperature tracer method the critical parameter for a reach scale recharge estimate is the wetted channel area which was estimated using KINEROS. Because of the small wetted channel width (15% of channel width), plausible variations of this parameter (10 to 50%) will result in recharge estimates ranging from ~50% lower to ~250% higher. While these parameters introduce high levels of uncertainty, it is important to note that this reflects, in part, the limited data collection. By focusing data collection on one method and focusing on the most uncertain aspect (Table 4) errors should be substantially improved.

While recharge estimates are in general agreement, some important differences between methods should be noted. First, results from the water balance approach produced the highest recharge rates. One reason for the high recharge value may be related to the temporal scale of the reach water balance compared to other methods. Various components of the reach water balance are measured or computed on an event or daily basis and then scaled up to a year. Other methods integrate over some period of time; for example, micrometry and the groundwater mound model integrate over the residence time of water in the vadose zone. The longer temporal scale of these methods result in recharge estimates that reflect both high runoff years (1999–00 and 2000–01) and to some extent years prior when recharge was lower. In contrast, the reach water balance will only reflect the study years (1999–00 and 2000–01), which had high runoff. Other reasons why the reach water balance might yield a high recharge estimate could be related to errors associated with individual components. Because the inputs and outputs to the reach are well measured at flumes 1, 2, and 7, the high values could be the result of an overestimate of modeled lateral inflow or an underestimate of near channel evapotranspiration. If one wants to ignore the difficulty of estimating near-channel transpiration, channel evaporation, and channel precipitation, a simplified estimate of recharge can be obtained by subtracting reach outflow (flume 1) from reach inflow (flume 2 + flume 7, Table 3, column 3).

In contrast to the reach water balance, the chloride mass balance method produced a lower recharge estimate. This

might be expected because additional Cl sources in the vadose zone and groundwater would result in artificially low recharge volumes. Additionally, the lower recharge estimates may reflect a multiyear residence time of groundwater such that it integrates over periods of high recharge (such as 1999 and 2000) and prior periods when recharge was lower. The Hantush groundwater mound model produces the lowest recharge rates. It is not clear why this is the case, however the variability of parameter sets derived from nearly adjacent wells indicates that small-scale aquifer heterogeneity, common in alluvial dominated areas, could lead to highly variable estimates.

The wider applicability of these methods can be considered based on two factors: the type/amount of data necessary, and the difficulty in evaluating and interpreting the data. The reach water balance method provides a conceptually simple approach to quantifying ephemeral channel recharge. However, quantifying all inputs and outputs can be expensive and challenging. The instrumentation in the WGEW is not easily replicated. The specially designed supercritical flumes, required for accurate discharge measurements for ephemeral channels with a mobile bed, are massive and expensive structures. Likewise, vadose zone temperature modeling necessitates substantial field work and lab analysis for vadose zone characterization and yields only infiltration rates. Although integrated temperature sensors and data loggers are now relatively cheap, more of them would be required at sites outside of the WGEW to obtain estimates of flow duration and the area of alluvial channel inundated by runoff [*Coes and Pool*, in review] in order to scale well-based vadose model results to the reach or basin scale. The data requirements for the reach water balance and vadose zone temperature modeling imply that these methods are not likely to be the best choices if recharge estimates are the only measure of interest. In contrast, the advantage of these methods is that they yield information on an event basis, allowing for processes-level understanding.

Other methods, because they integrate over some spatial and temporal scales, require significantly less data. For example, the chloride mass balance is conceptually simple and the calculation borders on trivial. It is encouraging to note that the simplified chloride mass approach balance, requiring more widely available observations, provides reasonable recharge estimates when compared to the more complicated or data intensive methods. Sample collection is straightforward and concentrations can be measured at a commercial lab. However, distinguishing “ephemeral channel recharge” groundwater from regional groundwater is a significant problem and, if not approached with caution,

will result in incorrect groundwater chloride values and drastic underestimates of ephemeral channel recharge. In terms of data collection, the Hantush groundwater mound model maybe the simplest; all that is needed is a groundwater well near the stream channel that is equipped with a pressure transducer and data logger. The microgravity method is very encouraging but relatively new. The microgravity change measurements are less prone to small-scale heterogeneity as they sense storage changes in a relatively large volume as compared to a well. While they do not require intrusive measurements, rather involved and subtle methods for data analysis and interpretation are required. In addition, this methods requires additional labor as repeat (~quarterly) site visits and measurements with a portable relative gravity meter are needed.

When applying methods that rely on data from groundwater wells, such as microgravity, groundwater mound modeling, and Cl mass balance, it is best to employ a set of wells aligned in a transect rather than a single well. A single well may not be representative or directly connected to ephemeral channel recharge. For example, the results of this study indicated that well 73 was not directly connected to ephemeral channel recharge and a substantial portion its water was derived from the regional groundwater aquifer. If only this well had been used, substantially different recharge rates would have been estimated. The reason we were able to identify well 73 was because we had multiple wells aligned in a transect. Identification of well 73 would have been aided by extending the transect from the stream channel to reach an interdrainage region that is not influenced by ephemeral channel recharge. When resources are limited, the well closest to the stream channel should be chosen as it most likely has the greatest connection to groundwater derived from ephemeral channel recharge.

4.7 Importance of Ephemeral Channel Recharge at the Basin Scale

To scale recharge estimates from the flume 2 and 7 to flume 1 reach scale, to the San Pedro Basin to the Tombstone USGS gage, simple geometric measures based on available GIS data were used. All the channels in the basin that had a drainage area equal to that of Flume 2 (~114 km²) were delineated using GIS software. The total length of these channels, excluding the main stem of the San Pedro, was then computed (152,500 m). The resulting ratio of channel lengths between the study reach and channels with a similar supporting drainage area in the San Pedro is 21.8. Using the very gross assumption that all the larger channels in the San Pedro behave similarly to WGEW study

reach and that they are exposed to a comparable climate and runoff regime, this ratio was used to compute total basin recharge estimates from ephemeral channel runoff losses for 1999–00 to 2000–01 totals for the minimum and maximum values in Table 3. The resulting estimates range from 6.8 to 19.3 million m³.

To put these numbers in context, under pre-pumping steady state conditions Corell et al. [1996] estimated total annual basin recharge to be approximately 23.2 million m³ (46.4 million m³ for two years). If the estimated recharge values in Table 3 scaled up to the San Pedro are even approximately correct it is fair to conclude that ephemeral channel recharge from monsoon runoff can be a substantial percentage of overall basin recharge (15% to 40%). Although these estimates are very crude, their relative magnitude as compared to overall basin recharge indicates that this mechanism for recharge should not be ignored in modeling and monitoring of the Upper San Pedro Basin water budget.

CONCLUSIONS

Recharge estimates from all methods agreed within a factor of three. This is a relatively good agreement, given the level of uncertainty associated with each method and the limited data collected. Individual methods yielded important results. The reach water balance revealed the limited size of ET losses (~20%) and limited area of inundated channel. For the Cl mass balance method, [Cl]/[SO₄] ratios were found to be useful for distinguishing ephemeral channel recharge from regional groundwater. In terms of wider applicability, the data requirements for reach water balance and vadose zone temperature modeling will limit their use for recharge estimates. However, because data for these methods is collected on an event basis, they will yield process level insights. In contrast, methods that integrate over time and space, such as microgravity, groundwater mound modeling, and Cl mass balance will find wider applicability for estimating ephemeral channel recharge. An important consideration for these methods is that data collection should be organized along a transect of wells that stretches across the stream channel from regional aquifer to right under the channel.

Another primary purpose of this study was to assess whether recharge from ephemeral channels was a significant component of the overall San Pedro Basin water budget (Walnut Gulch is a tributary to this basin). If one crudely scales recharge estimates from 1999 and 2000 to the overall length of channel in the basin, basin wide ephemeral channel recharge would be between 15% and 40% of the total

steady state recharge as estimated from a regional groundwater model [Corell *et al.* 1996]. It is important to note that 1999–00 and 2000–01 represent the wet extremes of ephemeral channel flow; in contrast, 2001 and 2002 had limited flow and no discernable deep recharge. Nevertheless, if the estimated recharge values are even approximately correct, then during years with significant monsoon runoff, ephemeral channel recharge can constitute a substantial percentage of overall basin recharge.

Acknowledgments. The authors would like to gratefully acknowledge Allon Owen for initiating this study and for the generous financial support of Cochise County, Arizona, the Upper San Pedro Partnership, and additional financial support from the Arizona Water Resources Research Center. In addition, this material is based upon work supported in part by SAHRA (Sustainability of semi-Arid Hydrology and Riparian Areas) under the STC Program of the National Science Foundation, Agreement No. EAR-9876800. This support is gratefully acknowledged. Special thanks are extended to the ARS staff located in Tombstone and Tucson, Arizona for their diligent efforts to collect long-term, high-quality data on the Walnut Gulch Experimental Watershed. The manuscript was substantially improved by the comments of Stan Leake, Bridget Scanlon and an anonymous reviewer. The authors wish to recognize the editorial assistance of Mary Black and manuscript preparation assistance of Cheryl Fusco and Mary White.

REFERENCES

- Allison, G.B., G.W. Gee, and S.W. Tyler, Vadose-zone techniques for estimating groundwater recharge in Arid and Semiarid Regions, *Soil Sci. Soc. Am. J.*, 58, 6-14, 1994.
- Barrett, D.J., T.J. Hatton, J.E. Nash, and M.C. Ball, Evaluation of the heat pulse velocity technique for measurement of sap flow in rainforest and eucalypt forest species of southeastern Australia, *Plant Cell Environ.*, 18, 463-469, 1995.
- Becker, P., and W.R.N. Edwards, Corrected heat capacity of wood for sap flow calculations, *Tree Physiol.*, 19, 767-768, 1999.
- Blash, K., T.P.A. Ferré, J. Hoffmann, D. Pool, M. Bailey and J. Cordova, Processes controlling recharge beneath ephemeral streams in southern Arizona, in *Recharge and Vadose-Zone Processes: Alluvial Basins of the Southwestern United States*, edited by F.M. Phillips, B.R. Scanlon and J.F. Hogan, 2004.
- Burgess S.S.O., M.A. Adams, N.C. Turner, C.R. Beverly, C.K. Ong, A.A.H. Khan and T.M. Bleby, An improved heat pulse method to measure slow and reverse flow in woody plant, *Tree Physiol.* 21, 589-598, 2001.
- Cienciala, E, J. Kucera, and A. Malmer, Tree sap flow and stand transpiration of two Acacia mangium plantations in Sabah, Borneo, *J. Hydrol.*, 236, 109-120, 2000.
- Cohen, Y., F. Fuchs, and D.C. Green, Improvement of the heat pulse method for determining sap flow in trees, *Plant Cell Environ.*, 4, 391-397, 1981.
- Coes, A.L., and D.R. Pool, Ephemeral-channel and basin-floor infiltration in the Sierra Vista subwatershed of the Upper San Pedro Basin, Southeastern Arizona. *U.S. Geol. Surv. Water-Resour. Invest. Rep.*, in review.
- Constantz, J., S.W. Tyler, and E. Kwicklis, Temperature-profile methods for estimating percolation rates in arid environments, *Vadose Zone J.*, 2, 12-24, 2003.
- Constantz, J., and C.L. Thomas, The use of streambed temperature profiles to estimate the depth, duration, and rate of percolation beneath arroyos, *Water Resour. Res.*, 32, 3597-3602, 1996.
- Corell, S.W., F. Corkhill, D. Lovvik, and F. Putman, A groundwater flow model of the Sierra Vista subwatershed of the Upper San Pedro Basin—Southeastern Arizona. *Arizona Department of Water Resources, Hydrology Div., Modeling Report No. 10.* Phoenix, Arizona, 107 pp., 1996.
- Dincer, T., A. Al-Mugrin, and U. Simmermann, Study of the infiltration and recharge through sand dunes in arid zones with special reference to the stable isotopes and thermonuclear tritium, *J. Hydrol.*, 23, 79-109, 1974.
- Dettinger, M.D. Reconnaissance estimates of natural recharge to desert basins in Nevada, USA, by using chloride-balance calculations, *J. Hydrol.*, 106, 55-78, 1989.
- Eriksson, E., and V. Khunaksem, Chloride concentration in groundwater, recharge rate and rate of deposition of chloride in Israel Coastal Plain, *J. Hydrol.*, 7, 178-197, 1969.
- Gatewood J.S., T.W. Robinson, B.R. Colby, J. D. Hem, L.C. Halpenny, The use of water by bottom-land vegetation in Lower Safford Valley, Arizona, *U.S. Geol. Surv. Water Supply Paper 1103*, 210 pp., 1950.
- Goodrich, D.C., Geometric simplification of a distributed rainfall-runoff model over a range of basin scales, Ph.D. Thesis, University of Arizona, 361 pp., 1990.
- Goodrich, D.C., T.J. Schmutge, T.J., Jackson, C.L., Unkrich, T.O., Keefer, R., Parry, L.B. Bach, and S.A. Amer, Runoff simulation sensitivity to remotely sensed initial soil water content. *Water Resour. Res.* 30,1393-1405, 1994.
- Goodrich, D.C., L.J. Lane, R.A. Shillito, S.N. Miller, K.H. Syed, and D.A. Woolhiser, Linearity of Basin Response as a Function of Scale in a Semi-Arid Watershed, *Water Resour. Res.* 33, 2951-2965, 1997.
- Goodrich, D.C., C.L. Unkrich, R.E. Smith, and D.A. Woolhiser, KINEROS2 - A distributed kinematic runoff and erosion model, *Proc. of the Second Federal Interagency Hydrologic Modeling Conference*, Las Vegas NV, 12 p., 2002.
- Hantush, M.S., Growth and Decay of Groundwater-Mounds in Response to Uniform Percolation. *Water Resour. Res.*, 3, 227-234, 1967.
- Healy, R.W., and A.D. Ronan, Documentation of computer program VS2DH for simulation of energy transport in variably saturated porous media—Modification of the U.S. Geological Survey's computer program VS2DT, *U.S. Geol. Surv. Water-Resour. Invest. Rep.* 96-4230, 36 pp., 1996.
- Heilweil, V.M., and D.K. Solomon, Millimeter- to Kilometer-Scale Variations in Vadose-Zone Bedrock Solutes: Implications for Estimating Recharge in Arid Settings, in *Recharge and Vadose-*

- Zone Processes: Alluvial Basins of the Southwestern United States*, edited by F.M. Phillips, B.R. Scanlon and J.F. Hogan, 2004.
- Lane, L.J., Chapter 19: Transmission losses, in *SCS National Engineering Handbook*, pp. 19-1 - 19-21, U.S. Gov. Printing Office, Wash., D.C., 1983.
- Libby, F. J., Wallace, D. E., Spangler, D. P., Seismic Refraction Studies of the Subsurface Geology of the Walnut Gulch Experimental Watershed, AZ, *USDA-ARS Report 41-164*, 14 pp., 1970.
- Mathieu, R., and T. Bariac, An isotopic study (H and O) of on water movements in clayey soils under a semiarid climate, *Water Resour. Res.*, 32, 779-789, 1996.
- Miller, S.N., D.J. Semmens, R.C. Miller, M. Hernandez, D.C. Goodrich, W.P. Miller, W.G. Kepner, and D. Ebert, GIS-Based hydrologic modeling: The automated geospatial watershed assessment tool, *Proc. of the Second Federal Interagency Hydrologic Modeling Conference*, Las Vegas NV, 12 p., 2002.
- Moench, A.F. and Kisiel C.C., Application of the Convolution Relation to Estimating Recharge from an Ephemeral Stream, *Water Resour. Res.*, 6, 1087-1094, 1970.
- Phillips, F. M., Environmental tracers for water movement in desert soils of the American Southwest, *Soil Sci. Soc. Am. J.*, 58, 15-24, 1994.
- Plummer, L. N., Bexfield, L. M., Anderholm, S. K., Sanford, W. E. & Busenberg, E. Using geochemical data and aquifer simulation to characterize recharge and groundwater flow in the Middle Rio Gradne Basin, USA, in *Recharge and Vadose-Zone Processes: Alluvial Basins of the Southwestern United States*, edited by F.M. Phillips, B.R. Scanlon and J.F. Hogan, 2004.
- Pool, D.R. and A.L. Coes, Hydrogeologic investigations of the Sierra Vista subbasin of the Upper San Pedro River basin, Cochise County, Southeast Arizona, *U.S. Geol. Surv. Water-Resour. Invest. Rep.*, 99-4197, 41 pp. and 3 sheets, 1999.
- Pool, D.R. and J.H. Eychaner, Measurements of aquifer-storage and specific yield using gravity surveys, *Ground Water*, 33, 425-432, 1995
- Pool, D.R., and W. Schmidt, Measurements of ground-water storage change and specific yield using the temporal gravity method near Rillito Creek, Tucson, Arizona: *U.S. Geological Survey Water-Resources Investigations Report 97-4125*, 30 p, 1997
- Rawls, W. J., D.L., Brakensiek, and K.E. Saxton, Estimation of soil water properties, *Transactions of the American Society of Agricultural Engineers*, Vol. 25 SW, pp. 1316-1320, 1328, 1982.
- Renard, K.G., L.J. Lane, J.R. Simanton, W.E., Emmerich, J.J. Stone, M.A. Weltz, D.C. Goodrich, and D.S. Yakowitz, Agricultural impacts in an arid environment: Walnut Gulch case study, *Hydrol. Sci. Tech.*, 9, 145-190, 1993.
- Rozanski, K., Araguás-Araguás, L., and R. Gonfiantini, Isotopic patterns in modern global precipitation, in *Climate Change in Continental Isotopic Records*, edited by P.K. Swart, K.L. Lohmann, J. McKenzie, and S. Savin, Geophysical Monograph 78, American Geophysical Union, Washington, DC, 1-37, 1993.
- Scanlon, B.R., Evaluation of moisture flux from chloride data in desert soils, *J. Hydrol.*, 128, 137-156, 1991.
- Scanlon, B.R., R.S. Goldsmith, and J.P. Paine, Analysis of localized unsaturated flow in fissured sediments in the Chihuahuan Desert, Texas: implications for contaminant transport. *J. Hydrol.*, 203, 58-78, 1997.
- Scanlon, B.R., R.P. Langford, and R.S. Goldsmith, Relationship between geomorphic settings and unsaturated flow in an arid setting, *Water Resour. Res.* 35, 983-999, 1999.
- Scanlon, B.R., K.Keese, R.C. Reedy, J. Simunek, and B.J. Andraski, Variations in flow and transport in thick desert vadose zones in response to paleoclimatic forcing (0-90 kyr): field measurements, modeling, and uncertainties. *Water Resour. Res.* 39, 1179; doi:10.1029/2002WR001604, 2003.
- Scott, R.L., W.J. Shuttleworth, T.O. Keefer, and A.W. Warrick, Modeling multiyear observations of soil moisture recharge in the semiarid Southwest, *Water Resour. Res.*, 36, 2233-2247, 1999.
- Scott, R.L., C. Watts, J. Garatuza, E. Edwards, D. Goodrich, D. Williams, W.J. Shuttleworth, The understory and overstory partitioning of energy and water fluxes in an open canopy, semiarid woodland, *Agric For. Meteorol.*, 114, 127-139, 2003.
- Scott, R.L., C. Watts, J. Garatuza, E. Edwards, D. Goodrich, D. Williams, W.J. Shuttleworth, The understory and overstory partitioning of energy and water fluxes in an open canopy, semiarid woodland, *Agric For. Meteorol.*, 114, 127-139, 2003.
- Shuttleworth, W.J., Chapter 4: Evaporation, in *Handbook of Hydrology*, edited by D. R. Maidment, McGraw-Hill, New York, 4.1 - 4.53, 1993.
- Smith R.E. and J.-Y. Parlange, A parameter-efficient hydrologic infiltration model, *Water Resour. Res.*, 14, 533-538, 1978.
- Smith, R.E., D.L. Chery, Jr., K.G. Renard, and W.R.Gwinn, Supercritical flow flumes for measuring sediment-laden flow, *USDA-ARS Tech. Bulletin No. 1655*, 70 pp., 1982.
- Smith, R.E., D.C. Goodrich, D.A. Woolhiser, and C.L. Unkrich, KINEROS—A Kinematic Runoff and Erosion Model, in *Computer Models of Watershed Hydrology*, edited by V.J. Singh, Water Resource Publications, Highlands Ranch, CO., pp 697-732, 1995.
- Sorey, M.L. and W.G. Matlock, Evaporation from an ephemeral streambed. *Journal of the Hydraulics Division. American Society of Civil Engineers*, January, 423-438, 1969.
- Stone, J.J., L.J. Lane, E.D. Shirley, and K.G. Renard, A Runoff-sediment Yield Model for Semiarid Regions, *Proc. 4th Fed. Interagency Sedimentation Conf.*, Las Vegas, NV, pp. 6-75 - 6-84, 1986.
- Swanson R.H, and D.W.A. Whitfield, A numerical analysis of heat pulse velocity and theory, *J. Exp. Bot.*, 32, 221-239, 1981.
- Taniguchi, M., and M.L. Sharma, Solute and heat transport experiments for estimating recharge rates, *J. Hydrol.*, 119, 57-69, 1996.
- Tromble J.M., Interception of rainfall by tarbush, *J. Range Mgmt*, 36, 525-526, 1983.
- Unland, H.E., A.M. Arain, C. Harlow, P.R. Houser, J. Garatuza-Payan, R.L. Scott, O.L. Sen, and W.J. Shuttleworth, Evaporation from a riparian system in a semi-arid environment, *Hydrol. Proc.*, 12, 527-542, 1998.

- Unkrich, C. and H.B. Osborn, Apparent abstraction rates in ephemeral stream channels, *Hydrology and Water Resour. in Arizona and the Southwest*, Office of Arid Land Studies, Univ. of Arizona, Tucson, 17:34-41, 1987.
- Wallace, D.E., L.R. Cooper, Dispersion of naturally occurring ions in groundwater from various rock types in a portion of the San Pedro River Basin, Arizona, *J. Hydrol.*, 10(4):391-405, 1970.
- Wallace, D.E., and D.P. Spangler, Estimating Storage Capacity in Alluvium by Gravity-Seismic Methods, *Bull. IASH*, 15, 91-104, 1970.
- Walvoord, M., A unifying conceptual model of water, vapor and solute movement in deep arid vadose zones, Ph.D. thesis, New Mexico Institute of Mining and Technology, 2002.
- Walvoord, M., F.M. Phillips, S.W. Tyler, and P.C. Hartsough, Deep arid system hydrodynamics, Part 2: Application to paleohydrologic reconstruction using vadose-zone profiles from the Northern Mojave Desert, *Water Resour. Res.*, 38, 1291, doi:10.1029/2001WR000925, 2002.
- Wood, W.W., and W.E. Sanford, Chemical and isotopic methods for quantifying ground water recharge in a regional, semiarid environment, *Ground Water*, 33, 458-468, 1995.
- Wood, W.W., K.A. Rainwater, and D.B. Thompson, Quantifying macropore recharge: Examples from a semi-arid area, *Ground Water*, 35, 1097-1106, 1997.
- Woolhiser, D.A., R.E. Smith, and D.C. Goodrich, KINEROS—A kinematic runoff and erosion model: Documentation and user manual, *USDA-ARS Pub. ARS-77*, 130 pp., 1990.
- Wright, W.E., δD and $\delta^{18}O$ in mixed conifer systems in the U.S. Southwest: The potential of $\delta^{18}O$ in *Pinus ponderosa* tree rings as a natural environmental recorder, Ph.D. thesis, University of Arizona, 328 p., 2001.
-
- Alissa L. Coes, U.S. Geological Survey, 810 Tyvola Road, Ste. 108, Charlotte, NC 28217.
- David C. Goodrich, USDA-ARS, 2000 E. Allen Rd., Tucson, AZ, 85719.
- James F. Hogan, Univ. of Arizona, Dept. of Hydrology and Water Resources, Tucson, AZ 85721.
- Kevin R. Hultine, Univ. of Arizona, School of Renewable Natural Resources, Tucson, AZ 85721.
- Scott Miller, Univ. of Wyoming, Dept. of Renewable Resources, Laramie, WY 82071.
- Don Pool, U.S. Geological Survey, 520 N. Park Ave., Suite 221, Tucson, AZ 85719.
- Russell L. Scott, USDA-ARS, 2000 E. Allen Rd., Tucson, AZ 85719.
- Carl L. Unkrich, USDA-ARS, 2000 E. Allen Rd., Tucson, AZ 85719.
- David G. Williams, Univ. of Wyoming, Dept. of Renewable Resources, Laramie, WY 82071.